

Corrosion Inhibition of Carbon Steel by Caprylate

By

Emmanuel Nwanebu

Department of Chemical Engineering
McGill University, Montreal

November 2015

A thesis submitted to McGill University in partial
fulfillment of the requirements for the degree of Master
of Engineering

© Emmanuel Nwanebu 2015

ABSTRACT

The aim of this project was to investigate the corrosion inhibition efficiency of an environmentally friendly molecule, sodium caprylate (SC), in protecting carbon steel (CS), used for production and short-range transport of crude oil, against internal corrosion in a media that contains aqueous (saline) phase.

Corrosion inhibition of CS in 3.5wt% NaCl solution by SC was investigated at different concentrations of SC using small amplitude cyclic voltammetry (SACV), electrochemical impedance spectroscopy (EIS), and Tafel polarization (TA) techniques. The corrosion inhibition efficiency data obtained from the three electrochemical methods were in excellent agreement.

Sodium caprylate was found to be a good inhibitor for CS, yielding a maximum corrosion inhibition efficiency of ca. 80% at 140mM inhibitor concentration. The corrosion inhibition efficiency was shown to be directly proportional to the surface coverage by SC. It was found that SC acts as a mixed-type inhibitor, by adsorbing on the CS surface, forming a self-assembled monolayer, and blocking both corrosion partial reactions (metal dissolution and hydrogen evolution). The adsorption of SC was found to follow the Langmuir adsorption isotherm. The apparent Gibbs free energy of adsorption calculated from the thermodynamic data was -23.8kJ/mol, indicating that the SC adsorption on the CS surface is highly spontaneous. The SC adsorption was found to follow the first-order reversible adsorption kinetics. It was also found that the adsorption equilibrium and the maximum corrosion inhibition efficiency was achieved after 30 minutes of adsorption.

SEM micrographs showed that the surface of the SC-inhibited CS was very much intact after 72 hours of exposure to the corrosive test media, while the surface of the uninhibited CS appeared to have deteriorated tremendously.

This study shows that SC is a good corrosion inhibitor for CS under the experimental conditions studied.

Résumé

Ce projet a pour but de rechercher l'efficacité de la molécule «vert» caprylate de sodium (SC) à protéger l'acier de carbone en inhibant de la corrosion interne dans les applications où il est en contact avec l'eau saline.

L'inhibition de la corrosion de l'acier de carbone dans une solution contenant 3.5% de chlorure de sodium par poids a été examinée utilisant l'inhibiteur SC à de différentes concentrations. Les techniques utilisés sont la voltampérométrie cyclique avec faible amplitude, la spectroscopie d'impédance, et la polarisation Tafel. Les données obtenues au sujet de l'efficacité de l'inhibition de la corrosion de tous les trois méthodes électrochimiques étaient en excellent accord.

Avec une efficacité maximum de ca. 80% à une concentration de 140mM d'inhibiteur, SC a été trouvé pour être un bon inhibiteur de l'acier de carbone. L'efficacité d'inhibition de la corrosion a été montrée pour être directement proportionnelle à la couverture de surface par SC. On a constaté que SC agit comme un inhibiteur du type mixte: elle s'adsorbe sur la surface de l'acier de carbone, forme une monocouche auto-assemblée, et puis bloque les deux réactions partielles de corrosion présentes (la dissolution du métal et le dégagement d'hydrogène). L'adsorption du SC suit l'isotherme d'adsorption de Langmuir. La fonction enthalpie libre G apparente calculé à partir des données était -23.8kJ/mol , ce qui indique que l'adsorption de SC sur la surface de l'acier de carbone est très spontanée. Également on a trouvé que l'adsorption suit une réaction réversible du premier ordre cinétique. Finalement, on a constaté que l'équilibre d'adsorption et l'efficacité maximale de l'inhibition de la corrosion ont été obtenus après 30 minutes.

Des micrographies parvenues de la microscopie électronique à balayage, démontre que la surface de l'acier de carbone exposé au SC était largement intact après 72 heures d'exposition aux médias de test corrosive tandis que la surface de la désinhibée acier semblait être détériorée considérablement.

Cette étude montre que le SC est un bon inhibiteur de corrosion pour de l'acier de carbone dans les conditions expérimentales étudiées.

ACKNOWLEDGEMENT

First and foremost, I thank Almighty God whose infinite mercies and grace endure forever. Also, with great joy, I express my sincere gratitude and appreciation to my thesis supervisor, Professor Sasha Omanovic, for his suggestions, research guidance, advice, immense wealth of knowledge and constant collaboration during this research project. He made it possible for the successful completion of this thesis. He literally carried me over the line on his shoulder.

Sweet mother, I dedicate this work to you for all you did to make today a reality for me and the entire Nwanebu and Uzoukwu family. You gave up your dreams and life so that we may have a better tomorrow. You will never be forgotten. God bless your gentle soul.

I would also like to thank my family especially my sister, Kelechi, who encouraged me and stood by me even when things got tough. I also would like to appreciate my Uncle, Jude, who provided me with the platform to springboard to success in my endeavors. Thank you.

My gratitude also goes to the McGill PRESSID scholars: Modupeola, Gbolahan, and Ademola among others. You always supported me to finish this work. Also, I would like to thank my friends and allies: Sarah, Simon, and Amardeep for being awesome friends. You are the true definition of friendship. Sarah, thank you for translating the thesis abstract from English to French. Jacob you are a special friend. Thanks for believing in me and helping me get through this one.

Special thanks to the Nigerian Government who through the National University Commission provided the financial backbone for my postgraduate study here at McGill University. I would also like to appreciate NSERC for providing the laboratory resources used for this research project.

Finally, I would like to thank everyone associated with my success story thus far. You all have helped to mold me to a better learned man today. God bless you all.

Table of Contents

ABSTRACT	ii
Résumé	iii
ACKNOWLEDGEMENTS	iv
Chapter 1: Introduction	1
Chapter 2: Background and Literature Review	4
2.1 Corrosion.....	4
2.1.1 Electrochemistry of Carbon Steel Corrosion.....	4
2.2 Forms of Corrosion.....	6
2.2.1 General (Uniform) Corrosion	7
2.3 Corrosion Mitigation Methods in the Oil and Gas Industry.....	7
2.3.1 Appropriate Selection of Materials	8
2.3.2 Cathodic Protection	8
2.3.3 Protective Coatings.....	8
2.3.4 Chemical Inhibitors	9
Chapter 3: Objectives	16
3.1 Main objectives.....	16
3.2 Specific objectives	16
3.3 Thesis Structure	16
3.4 Sodium Caprylate as choice of Inhibitor	17
Chapter 4: Methodology and Experimental Approach	19
4.1 Chemicals and solutions	19
4.2 Substrate Pretreatment	19
4.3 Experimental set up	20
4.4 Experimental Techniques and Equipment.....	21
4.4.1 Experimental Techniques	22
4.4.2 Experimental Equipment	25
Chapter 5: Results and Discussion	26
5.1 Corrosion inhibition by sodium caprylate (SC).....	26

5.1.1 Open Circuit Potential	26
5.1.2 Small Amplitude Cyclic Voltammetry (SACV).....	28
5.1.3 Electrochemical impedance spectroscopy (EIS)	32
5.1.3 Linear Tafel Polarization	40
5.1.4 SC configuration on the CS surface	43
5.1.5 SC adsorption isotherm and kinetics of SC adsorption.....	44
5.1.6 Scanning electron microscopy	49
Chapter 6: Conclusions and Future Work.....	51
6.1 Conclusions.....	51
6.2 Recommendations for Future Work	52
Reference.....	53

List of Figures

Figure 2. 1: Effect of oxygen concentration on corrosion of mild steel in slowly moving distilled water [8]. 5

Figure 2. 2: Effect of NaCl on corrosion of iron in aerated solutions at room temperature (composite of data from several investigators) [9]. 6

Figure 3. 1: sodium caprylate molecule (Sigma-Aldrich) 17

Figure 4. 1: Experimental setup 20

Figure 4. 2: Typical SACV current-potential loops for 90:10 Cu–Ni alloy in flowing seawater containing dissolved oxygen [35]. 23

Figure 5. 1: Variation of the open circuit potential (OCP) with time for CS electrode immersed in 3.5wt% NaCl, in the absence and presence of various concentrations of SC. (1) 0 mM, (2) 20 mM, (3) 50 mM, (4) 80 mM, and (5) 100 mM SC. Temperature = 296 ± 2 K. 27

Figure 5. 2a: Typical SACV current-potential voltammogram of a CS electrode in a saline environment at 296 ± 2 K. 28

Figure 5. 3a: Corrosion inhibition efficiency of CS derived from SACV measurements performed at various concentrations of SC in 3.5wt% NaCl solution. The data was obtained at 296 ± 2 K.... 31

Figure 5. 4: Nyquist plot of CS recorded at different SC concentrations in 3.5wt% NaCl solution. (●) 0 mM, (▲) 5 mM, (◆) 50 mM and (⊗) 140 mM SC. Symbols represent experimental data and solid lines depict the modeled spectra. The spectra were recorded at OCP after 2 hours of stabilization of the CS electrode at OCP. Temperature = 296 ± 2 K. 33

Figure 5. 5: Bode modulus impedance plots for CS recorded at various concentration of SC in the electrolyte and at OCP: (●) 0 mM, (▲) 5 mM, (◆) 50 mM and (⊗) 140 mM SC. Temperature, $T = 296 \pm 2$ K. Symbols represent experimental values, while solid lines depict simulated spectra. 35

Figure 5. 6: Bode plot for CS recorded at OCP in a 140mM SC solution of 3.5wt% NaCl measured at temperature, $T = 296 \pm 2$ K. Symbol (●) represent experimental values, while the solid line (—) depicts simulated spectra. 35

Figure 5. 7: EEC models used to fit EIS data recorded on (a) unprotected CS electrode (control sample), and (b) on a CS electrode immersed in 3.5wt% NaCl in the presence of SC. R_{el} – electrolyte resistance; CPE_1 – double-layer capacitance; R_1 – charge-transfer resistance, CPE_2 – adsorbed inhibitor layer pseudo-capacitance, R_2 – adsorbed inhibitor layer resistance. 37

Figure 5. 8: Corrosion inhibition efficiency of CS obtained from EIS measurements performed at different concentrations of SC in 3.5wt% NaCl solution and at OCP. The data was obtained at $T=296 \pm 2$ K. 39

Figure 5. 9: Comparison of the inhibition efficiency of SC on CS surface immersed in a 3.5wt% NaCl aqueous solution, obtained via EIS (●) and SACV (▲) measurements at 296 ± 2 K. 40

Figure 5. 10: Tafel plots of CS recorded in the (1) absence, and (2) presence of 50 mM of SC in the test solution performed at temperature, $T = 296 \pm 2$ K. Scan rate was 1 mV/s. 41

Figure 5. 11: A typical Tafel plot of CS electrode immersed in 3.5wt% NaCl illustrating the method of determining corrosion current i_{corr} 42

Figure 5. 12: Mean inhibition efficiency plot of CS immersed in 3.5wt% NaCl with various concentration of SC. Temperature, 296 ± 2 K. The inset represents the three different possible orientation of SC on the surface of CS. 43

Figure 5. 13: Linearized Langmuir adsorption isotherm for the adsorption of SC onto CS surface in a 3.5wt% NaCl solution. The data was recorded at $T= 296 \pm 2$ K. 46

Figure 5. 14: SC fractional surface coverage on CS obtained from SACV experiments performed in 3.5wt% NaCl solution containing 80 mM of SC, at 296 ± 2 K. Symbols represent experimental values, while the solid line represents the kinetic model, Eq. (5.7). 48

Figure 5. 15: SEM micrographs of CS surface: (a) after polishing (b) after 72h of immersion in uninhibited test solution (c) after 72h of immersion in 50mM SC (d) after 72h of immersion in 140mM SC. 49

List of Tables

Table 4. 1: Chemical composition of carbon steel rod.	21
Table 5. 1: OCP and polarization resistance values determined from SACV measurements performed with CS electrode in 3.5 wt% NaCl solutions without and with various concentrations of SC at 296 ± 2 K. The table also shows the corresponding corrosion inhibition efficiency.	30
Table 5. 2: Dependence of EEC parameters on the concentration of SC in the electrolyte. The data were obtained by modeling impedance spectra recorded at different concentration of SC in test solution at 296 ± 2 K and at OCP. The table also lists the corresponding corrosion inhibition efficiency values, ε_{std} = standard deviation. The average electrolyte resistance value was $11.2 \pm 0.8 \Omega$	38
Table 5. 3: Corrosion current values of CS in various concentration of SC in the test solution with corresponding corrosion efficiency recorded at $T = 296 \pm 2$ K.	42

Chapter 1: Introduction

Carbon Steel (CS) is one of the most frequently used construction materials because it is of a lower cost compared to other materials offering similar physico-chemical properties. However, if not properly protected, CS is susceptible to corrosion. Given sufficient time, in the presence of oxygen and water, Carbon Steel material will eventually change entirely to rust and disintegrate. Corrosion – commonly called rusting – is a microscopic process with huge impact on companies and individual consumers. Undoubtedly, corrosion has an enormous economic and environmental effect on virtually all facets of the world’s infrastructure, like bridges and buildings, oil and gas structures, chemical processing and highways structures, wastewater treatment systems etc. The costs associated with corrosion damage are indeed huge. For example, in the US it adds up to approximately 4.2 % of the Gross National Product (GNP), i.e. well over 400 billion dollars per year. These costs can be attributed to failure or deterioration of equipment, and the associated downtime, replacement and maintenance [1]. A recent estimate of the worldwide direct cost of corrosion – for prevention as well as repair and replacement – exceeded \$1.8 trillion (1.4 trillion euro; 12.2 trillion Yuan), or 3-4 % of GNP of industrialized countries [2]. Hence, the global community is faced with the challenge of providing means of combating this perennial, persistent problem in terms of design, material selection and material corrosion prevention/protection.

In addition to the economic significance, corrosion also poses large ecological and safety problems as a result of corrosion-caused damage to industrial and civil structures. In the Oil & Gas upstream production systems, corrosion is possibly the most significant and costly cause of severe operational problems. Corrosion can occur anywhere in the production line, from production wells to transporting vessels of produced gas or oil heading to the refineries. Because

corrosion is a natural occurring process, it is impossible to completely avert it. However, it can be controlled so that materials and equipment likewise can perform for a predicted optimum length of time. Hence, corrosion detection, monitoring and control become dominant considerations when seeking maximum equipment lifetime, minimum cost and maximum safety, in many industries. Therefore, it is necessary to first understand the nature and mechanisms by which corrosion occurs so as to minimize it. In the Oil & Gas industry specifically, the key reason for corrosion of CS is the presence of dissolved carbon dioxide CO_2 (sweet corrosion), hydrogen sulfide H_2S (sour corrosion) and oxygen in the oil that contains water, as well as dissolved sodium chloride, for example, in water injection wells and the use of acids during well acidizaion [3-5]. Removal of anyone of the above stated corrosion media might result in the corrosion slowdown.

There are several types of corrosion, such as general (uniform) corrosion, pitting corrosion, crevice corrosion, stress corrosion cracking, to name only a few. Of particular interest to the current project, is the general type of corrosion.

There are ample techniques used for decreasing a (general) corrosion rate of materials of construction, such as anodic/cathodic protection, applying protective polymer or metal coatings, better design of equipment, and corrosion inhibition by using chemicals, to name a few. Of particular interest for control of internal corrosion is the latter technique, which is based on the use of chemical compounds that are added in small quantities to the given corrosive environment to change the interaction of the metal with its corrosive environment. These compounds slow down the kinetics of the anodic corrosion reaction (metal dissolution) or of the cathodic corrosion reaction (oxygen or proton reduction), thus decreasing the overall rate of corrosion. Or, they adsorb on the substrate surface acting as a diffusion barrier for corrosive species, thus decreasing the rate of corrosion. On the other hand, to control the external corrosion, protective (usually

polymer) coatings are applied. Similarly to inhibitors, these coatings also act as a diffusion barrier for corrosive species, thus decreasing the rate of corrosion.

Current inhibitors used in many industries, and thus also in the Oil & Gas industry, are not environmentally friendly, and increasingly more stringent regulations are demanding their replacement by new “green” inhibitor molecules. Consequently, this thesis aims at contributing to the investigation of corrosion inhibition efficiency of an environmentally friendly molecule, caprylate, in protecting carbon steel against internal corrosion in the environment typical for production and short-range transport of crude oil.

Chapter 2: Background and Literature Review

2.1 Corrosion

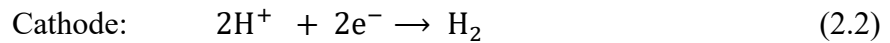
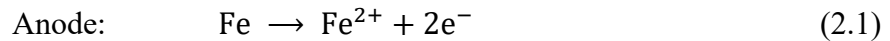
The term corrosion is the degradation of metal by chemical or electrochemical reactions as a result of its interaction with different environment leading to loss of integrity of the metallic structure. The term corrosion, from the technical point of view, is as old as the manufacturing industry and perhaps it is better appreciated when one recognizes that few thousand scientific and technical articles are released each year which deal directly or indirectly with corrosion and ways of combating and mitigating it.

2.1.1 Electrochemistry of Carbon Steel Corrosion

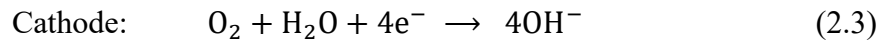
Corrosion being a chemical or electrochemical oxidation process entails the transfer of electrons between the metal and the environment (redox species in the electrolyte) in which the metals are either dissolved in the electrolyte, or converted to their oxides or other compounds that could also be dissolved or deposited on the metal surface as solids. The most common way of corrosion of metals is electrochemical. Considering that carbon steel (CS) is one of the most commonly used materials of construction, and is the metal considered in this graduate project, the emphasis in this section will be on the electrochemistry/corrosion of CS.

An electrolyte is analogous to a conductive solution, which contains positively and negatively charged ions. An ion is an atom that has lost or gained one or more outer electron (s) and carries an electrical charge. Thus, the corrosion process due to current flow, requires at least two reactions that must occur in a particular corrosive environment (e.g. 3.5wt.% NaCl aqueous solution). These reactions are classified as anodic and cathodic reactions [6]. For instance, a CS surface can be covered by a thin layer of water, containing some dissolved salts, thus providing

the electrolyte for electrochemical reactions. Given that the CS surface is not homogeneous, some sites on the surface will have higher surface energy than others, i.e. there will be cathodic (more noble) and anodic (less noble) sites on the CS surface, and there will, thus, be a potential difference between them, which represents the driving force for corrosion. In the absence of oxygen, ferrous ions are the primary anodic products of CS corrosion. At cathodes, hydrogen gas is formed:



However, in the presence of oxygen, the cathodic reaction is oxygen reduction:



It can be observed that both dissolved oxygen (or proton) and water are required for the corrosion process to proceed. The rate of corrosion of the steel product depends on the concentration of oxygen dissolved in the water at the steel surface, as shown in Figure 2.1. At low concentrations, the rate increases with increasing dissolved oxygen concentration. At high concentrations, the rate declines because of passivation [7].

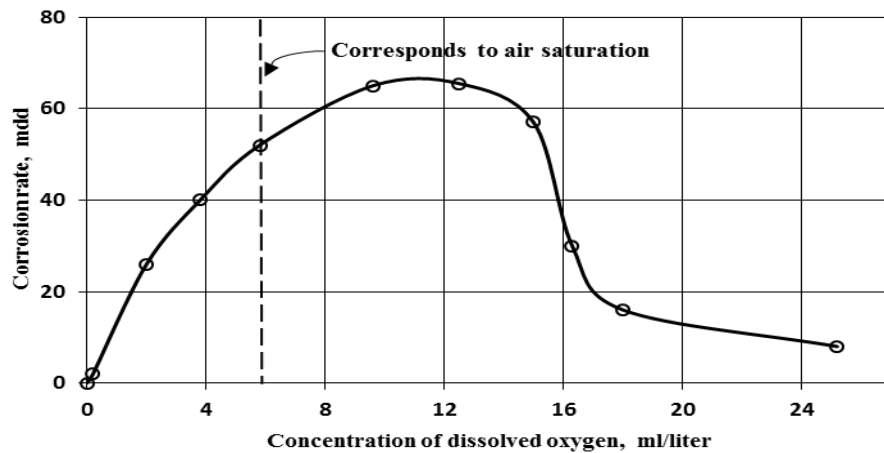


Figure 2. 1: Effect of oxygen concentration on corrosion of mild steel in slowly moving distilled water [8].

The corrosion rate can occur at a higher rate if the conductivity of the electrolyte increases. Typically dissolved salts increase conductivity. That is the main reason the presence of salts increases the rate of corrosion of CS. The relationship between NaCl concentration and corrosion rate is shown in Figure 2.2. The dashed vertical line in the figure indicates the salt concentration in seawater. At higher salt contents, the rate of corrosion decreases because the solubility of oxygen decreases as the NaCl concentration increases. Other factors like pH and temperature [7] and other dissolved salts [8] also impact the rate of corrosion.

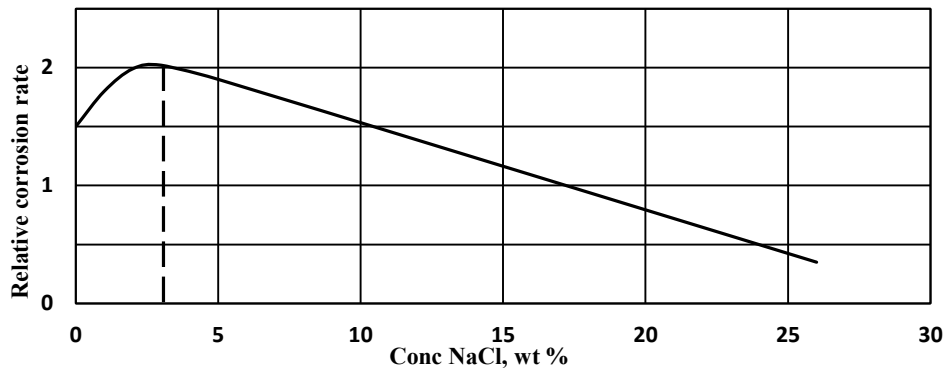


Figure 2. 2: Effect of NaCl on corrosion of iron in aerated solutions at room temperature (composite of data from several investigators) [9].

With the knowledge of all the aforementioned contributing factors to corrosion, it is possible to limit corrosion by precluding the direct molecular contact of oxygen and water from the surface of the carbon steel.

2.2 Forms of Corrosion

There are different forms of corrosion, such as general (uniform) corrosion, localized corrosion, erosion corrosion, to name a few. However, this graduate work focuses only on the general corrosion. Consequently, only general corrosion will be very briefly explained below.

2.2.1 General (Uniform) Corrosion

This form of corrosion takes place with equivalent intensity over the entire surface of the material. It is also referred to as the corrosion that proceeds at approximately the same rate over the exposed metal surface. Also, it is seen as the most serious form of corrosion on CS. Fortunately, it is the most well know type of corrosion and its rate can be predicted (determined) and taken into account when designing various structures. Some well-known examples include general rusting of steel and iron. Carbon steel corrodes uniformly when exposed to open atmospheres, sea-water, and soils to mention a few leading to the rusty appearance.

As mentioned above, uniform corrosion can be predicted, therefore, it can be taken into account when designing engineering structures by incorporating the necessary tolerance to carter for general corrosion by way of increasing the thickness of metallic structures. It is also possible to control this form of corrosion by painting, coating, or modifying the environment to become less corrosive, or by using chemical inhibitors which forms protective monolayers on the metal surface and thus insulate the surface form the corrosive environment.

2.3 Corrosion Mitigation Methods in the Oil and Gas Industry

The corrosion challenges in the oil fields are dynamic phenomena and those that are of highest concern. Hence, in order to improve the life span of structures in oil fields, corrosion needs to be fought to, at least the barest minimum. Although many methods have been highlighted in the past to combat corrosion on these offshore and onshore facilities, the mitigation methods can be classed broadly into the categories outlined below.

2.3.1 Appropriate Selection of Materials

It is important to understand that no single material is a cure for all the corrosion problems that exist, even in the oil industry. There is a need for detailed study of associated corrosion mechanisms, crude oil flow conditions, and the life expectancy of material before selecting a specific metal. Though expensive materials, like titanium, can operate in almost all corrosive environments, the required initial investment limits its use. Instead, carbon steel have found good use in seawater (and many other) environments because of its good mechanical properties and relative low cost. However, for situations where more corrosion resistant material is required, alternatives may be used, such as stainless steels, etc. Nevertheless, CS remains *the* material of choice not only in the oil and gas industry, but in many other industries.

2.3.2 Cathodic Protection

Cathodic protection is a technique based on the polarization of the material (to be protected) into the cathodic potential region, where it does not (thermodynamically) corrode. The method can be applied by either using sacrificial anodes or by means of more complex impressed current systems. The key difference between the two is that impressed current cathodic protection uses an external power source with inert anodes (e.g. graphite or metal-oxide anodes) while sacrificial anode cathodic protection uses the naturally occurring electrochemical potential difference that exists between different metallic elements to provide protection (e.g. between Mg or Zn and CS).

2.3.3 Protective Coatings

Coatings are thin materials applied as a liquid or powder which on solidification should be firmly and continuously attached to the material they protect from corroding. These materials may be organic or inorganic. It is important that coatings are flexible, resistant to chemical attack from surrounding fluids, strongly adhesive, have little or no pores, and show thermal stability. Coatings

can act as anti-corrosives, adhesives, anti-reflectives, catalysts, etc. The earliest report efforts to prevent fouling of surfaces date back to 412 BC when explorers coated the wooden hulls of ships with tallow and pitch poisoned with arsenic and sulfur to keep barnacles at bay [10]. Today, coatings are still very much in use and are typically used for control of external corrosion.

2.3.4 Chemical Inhibitors

One of the most common ways of limiting internal corrosion in the oil industry is through the use of chemical corrosion inhibitors [11, 12]. Corrosion inhibitors are chemicals which, when added in small quantities in the corrosive media, slow down corrosion of the metallic surface. These chemicals protect the surface of metals either by merging with them (physically via physisorption or chemically through chemisorption) or by reacting with the corrosion-participating compounds in the corrosive electrolyte [13]. A corrosion inhibitor may act in a number of ways: It can simply restrict the rate of the anodic process or cathodic process by forming a protective film that minimizes the interaction between the anodic or cathodic sites on the metal surface, respectively, and the surrounding corrosive environment. Alternatively, it may act by increasing the potential of the metal surface in such a way that the metal enters the passivation region where, for example, a natural oxide film forms. Another mode of action of inhibitors, which is the most common mode, is that the inhibiting compound blocks off all of the metal surface by adsorbing on them and ‘insulating’ them from the corrosive environment [13]. Also, it can simply change media characteristics, producing precipitates that can be protective and inactivating of an aggressive constituent [14]. An inhibitor is considered to be good if it is compatible with the environment, economical for application, and gives the required corrosion protection effect when present in small concentrations [15]. Most of currently used inhibitors are organic-based molecules.

2.3.4.1 Classification of chemical inhibitors

Inhibitors can be grouped into environmental conditioners and interface inhibitors. Environmental conditioners decrease the corrosivity of media by scavenging of corrosive species present in the surrounding (e.g. dissolved oxygen). Hence, these inhibitors are called scavengers [15]. On the other hand, interface inhibitors mitigate corrosion by forming a film at the metal/surrounding interface. Interface inhibitors can be further classified into liquid- and vapor-phase inhibitors. Of the aforementioned two, liquid-phase inhibitors are of key importance and can be classified as anodic, cathodic, or mixed inhibitors, depending on whether they inhibit the anodic, cathodic, or both electrochemical reactions respectively [15].

Currently, mixed corrosion inhibitors are most-frequently used inhibitors. They are mostly organic compounds that work by affecting the kinetics of both the anodic and cathodic corrosion reactions. These inhibitors protect by adsorbing on the metal (corroding) surface. This could be through physical adsorption (physisorption), chemical adsorption (chemisorption) or both of them, which is believed to depend on the structure of the inhibitor, surface physico-chemical properties of the metal (charge, wettability, chemical reactivity), and electrolyte type [15, 16]. Organic inhibitors have been the most widely used inhibitors in the oil industry (including petroleum processing) because of their ability to form a protective layer on the metal surface in media with high hydrocarbons content [14].

2.3.4.2 Choice of corrosion inhibitor

In literature, many reports have correlated the substituent effect and the inhibitory efficiency of molecules based on nitriles, pyridines, anilines, imidazolines, polyesters, aliphatic amines, benzoic acid, sulfides, thiophenes etc. The use of inhibitors based on these aforementioned molecules is as result of their mechanism of action, such as their electron-donating ability.

Therefore, selecting the right organic inhibitor for a specific environment and metal must be done with great care as no single inhibitor is known to protect all metals in different corrosive environments. In order to choose a good corrosion inhibitor, one must consider the following:

- It should be synthesized conveniently from relatively cheap raw materials or cost-effectively extracted from natural resources [17, 18].
- Elements like oxygen, nitrogen, phosphorus, sulfur and the presence of multiple bonds or aromatic rings in the inhibitor molecule is preferred as this leads to increased adsorption of the compound on the metal surface and therefore to the enhancement of inhibition efficiency [17, 19]. The inhibition efficiency, in the most general and primitive approximation, follows this sequence: $O < N < S < P$ [20].
- It should be compatible with the system fluids, system conditions and other chemicals in the system.
- It should not have side effect [14], and should neither be toxic nor pose health risk to operators and maintenance personnel [21].
- It should be environmentally friendly (green). When discharged as an effluent, it should have low or zero environmental impact [22, 23].

2.3.4.3 Toxic Effect of Chemical Inhibitors

In the oil industry, the use of corrosion inhibitors has become a common practice. However, some of these chemicals cause harm to the environment. Many common corrosion inhibitors that are still in use, are very toxic and/or environmentally unfriendly [24]. A number of currently-used inhibitors contains chromates (these are forbidden in most developed countries), which are believed to be carcinogenic [24, 25]. Therefore, it is important to find inhibitors that are non-hazardous, but could protect metals against corrosion at high corrosion efficiency. Consequently,

it is paramount to study environmentally-friendly molecules that could potentially be used as corrosion inhibitors. For example, molecules which form ordered self-assembled monolayers on (to-be-protected) surfaces are of key interest as possible corrosion inhibitors.

2.3.4.4 Environmentally-friendly Corrosion Inhibitors

As a result of the toxicity engendered by many currently-used chemical, there is an increasing need to develop more environmentally-friendly corrosion inhibitors. Safety and environmental concerns have become heightened in the oil (but also many other) industry operations. Therefore, extensive research is currently undertaken both in the industry and the academia, to answer to this need. For example, Omanovic *et al.* [26] studied the electrochemical behavior of austenitic low carbon stainless steel (316L) in the presence of sodium salt of linoleic acid (inhibitor) in a phosphate buffer solution; they found that this inhibitor gave high corrosion inhibition efficiency (ca. 95%) and has the potential to be used as an environmentally friendly corrosion inhibitor. The Omanovic lab has also studied a possibility of using 12-aminododecanoic acid anion as corrosion inhibitor of CS in a range of environments, and they have concluded that the molecule can efficiently protect CS from uniform corrosion by adsorbing on the CS surface and “insulating” it from the corrosive environment. Also, de Souza and Spinelli [27] have studied the inhibitory effect of a naturally occurring biological molecule, caffeic acid, considered as a green corrosion inhibitor, for mild steel in 0.1 M H₂SO₄. They showed that caffeic acid is a good corrosion inhibitor for mild steel in the acidic electrolyte, yielding a maximum inhibition efficiency of ca. 96%. The work of Barakat *et al.* [28] has shown that the corrosion inhibition offered by water extracts of coumarines, and fatty extracts of some Egyptian plants to corrosion of mild steel in NaCl was substantial. These cheap extracts gave higher inhibition efficiency in the presence of H₂S (which is the primary cause of hydrogen attack in *sour* corrosion). Moretti *et al.*

[22] studied the use of tryptamine as a green iron corrosion inhibitor in 0.5 M deaerated H₂SO₄. Tryptamine, a derivative of tryptophan, is one of the standard amino acids. It is relatively cheap, non-toxic and easy to make in purity greater than 99%. At a concentration of 10 mM, it was found to be an effective iron corrosion inhibitor, even at 55 C° for a period of 72+ hr. Furthermore, Quraishi *et al.* [29] synthesized a macrocyclic compound, tetramethyl-dithia-octaazacyclotetradeca-hexaene (MTAH), in order to study its inhibiting effect on pickling of mild steel in 20% H₂SO₄ at 95°C. The results show that in the presence of potassium iodide as a synergent, the corrosion inhibition efficiency was increased up to ca.99.9%. MTAH was chosen because (i) it contains 10 heteroatoms (8 nitrogen and 2 sulfur) as reactive centers for easy adsorption on the metal surface, (ii) it is readily soluble in the medium, and (iii) it does not pose health hazards like other thiourea derivatives that have been commonly used as corrosion inhibitors.

2.3.4.5 Adsorption of corrosion inhibitors

The primary mechanism of corrosion inhibition by organic inhibitors is through adsorption of inhibitor molecules onto the (protected) corroding metal surface. The adsorbate (inhibitor) serves as a mass-transfer barrier to isolate the corrosion-susceptible metal from the corrosive media. This protective action is often associated with chemical and/or physical adsorption. Chemisorption involves the formation of chemical bonds by sharing of electrons between the metal and the adsorbate. On the other hand, physisorption is a type of adsorption in which the forces involved are intermolecular forces (e.g. van der Waals, electrostatic, hydrogen-bonding forces) which do not result in a significant change in the electronic orbital patterns of the species involved. Chemisorption has a higher heat of adsorption or activation energy than electrostatic adsorption as it entails new bond formation, hence it is typically irreversible. It is believed to occur through donation of electrons from species with loosely bonded electrons, like π -electrons

in aromatic rings, or multiple bonds, or unpaired electrons in functional groups of the inhibitor that contain atoms of O, N, S, or P, to the empty d-orbital of a transition metal, in the case of CS, iron [30, 31]. The corrosion inhibition efficiency of organic inhibitors is, in the most general case,

It is important to note that adsorption isotherms are useful in understanding the mechanism of inhibition of corrosion reaction of metals/alloys. There are a range of isotherms that could be used to describe the adsorption of an inhibitor molecule on a metal surface. These include the Langmuir, Temkin, Frumkin, Florry-Huggins, Virial Parson, Temkin, and Bockris-Swinkles isotherms, to name a few. The most commonly used of them all is the Langmuir adsorption isotherm [19, 31, 32] as it gives a good fit for isotherms of physical or chemical adsorption. The Langmuir adsorption isotherm relates the equilibrium concentration (c , mol dm⁻³) of the adsorbate in the bulk solution to the degree of surface coverage, θ , according to the equation:

$$\frac{c}{\theta} = \frac{1}{B_{ads}} + c \quad (2.4)$$

where B_{ads} (dm³ mol⁻¹) is the equilibrium adsorption constant which reflects the affinity of the adsorbate molecules toward adsorption sites. This parameter B_{ads} evaluated at a constant temperature could be defined by [26, 33]:

$$B_{ads} = \frac{1}{c_{solvent}} \exp\left(\frac{-\Delta G_{ads}}{RT}\right) \quad (2.5)$$

where R (J mol⁻¹K⁻¹) is molar gas constant, T (K) is the temperature, ΔG_{ads} (J mol⁻¹) is the Gibbs free energy of adsorption and $c_{solvent}$ is the molar concentration of solvent (in aqueous solutions, water; 55.5 mol dm⁻³). When the Gibbs free energy is evaluated at various temperatures, the adsorption enthalpy can be calculated by the equation given below, assuming the adsorption mechanism is constant within the temperature range investigated:

$$\Delta G_{ads} = \Delta H_{ads} - T\Delta S_{ads} \quad (2.6)$$

With equation (2.6) it is possible to know the driving force for the adsorption process and the adsorption bond strength. For a good inhibitor, the Gibbs free energy should be negative signifying that the adsorption process is spontaneous; the absolute value of ΔG_{ads} indicates the degree of the 'spontaneity' of the process. Omanovic and Roscoe [26] used the Langmuir isotherm to describe the adsorption of sodium salt of linoleic acid (LA) on stainless steel in a phosphate buffer solution. ΔG_{ads} of LA adsorption at 299 K was calculated to be $-43.3 \text{ kJ mol}^{-1}$, which indicated highly spontaneous adsorption of LA. Also, Omanovic and Ghareba [34] studied the adsorption of a sodium salt of 12-Aminododecanoic acid (AA) on carbon steel and correlated the result with Langmuir isotherm. Their results show that the standard Gibbs free energy of adsorption of AA on the CS surface at 295 K was $-26.3 \text{ kJ mol}^{-1}$. This quite negative value demonstrates that the AA adsorption process is highly spontaneous.

Chapter 3: Objectives

3.1 Main objectives

There is a growing need to fight corrosion with more environmentally-friendly inhibitors and to investigate their possible use under various experimental conditions mimicking those in real applications. For this research project, the major goal is to investigate a possibility of an environmentally friendly molecule, caprylate, in protecting carbon steel against internal corrosion in a media prevalent for production and short-range transport of crude oil that contains an aqueous (saline) phase.

3.2 Specific objectives

(1) The key objectives will be met by addressing the following specific objectives:

Investigation of the corrosion inhibition efficiency of caprylate in protecting carbon steel from general corrosion in a saline electrolyte.

(2) Investigation of the adsorptive interaction of caprylate with a carbon steel surface.

(3) Investigation of the kinetics of adsorption of caprylate on carbon steel in saline environment.

3.3 Thesis Structure

- Chapter 1 highlights corrosion problem and its economic implication and states methods of corrosion control with emphasis on "green" inhibition.
- Chapter 2 addresses carbon-steel general corrosion mechanism. Then presents background information on corrosion inhibitors, how they work and their selection criteria with accent on the use of environmentally-friendly corrosion inhibitors.

- Chapter 3 states the main and specific objectives of the thesis.
- Chapter 4 describes the general experimental materials, methods and procedures used for the project.
- Chapter 5 covers detailed presentation on all obtained results with accompanying discussion
- Chapter 6 concludes the thesis by summarizing major findings from results presented and gives a brief of possible future work that can emanate from the research project.

3.4 Sodium Caprylate as choice of Inhibitor

As stated in the previous chapter, there is an increased need to design and develop environmentally friendly organic molecules that could serve as corrosion inhibitors. Carboxylates (e.g. amino or fatty acids) have been shown to be good candidates, and those with a long hydrophobic alkyl chain and hydrophobic methyl end-group are more attractive. These molecules could form self-assembled-monolayers (SAMs) which in turn leads to increased corrosion inhibition efficiency through hydrophobic activities (they represent a barrier for transport of hydrated corrosive species from the bulk electrolyte to the metal surface). After studying different alkyl-carboxylate molecules, sodium octanoate, otherwise known as sodium caprylate (SC), was chosen as chief candidate (see Figure 3.1).

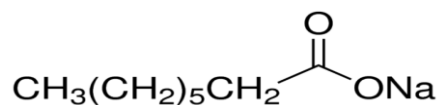


Figure 3. 1: Sodium caprylate molecule.

This molecule is indeed environmentally friendly. It has been commonly used as protein stabilizer for molecules such as fibrinogen. It comprises a 7-carbon alkyl chain, which is enough

of C atoms to form a semi-ordered SAM. When longer alkyl-chain molecules were initially considered (C10, C12 and C18), they proved to be less soluble in aqueous solution. Sodium caprylate contains a methyl group which in combination with the aforementioned alkyl-chain serves as a hydrophobic-barrier for the permeation of water and charged species. Its carboxylate head-group is polar, and yields high electron-density around oxygen atoms, thus making it a good adsorption-group. Consequently, sodium octanoate should provide high corrosion inhibition efficiency for carbon steel in sea-water.

Chapter 4: Methodology and Experimental Approach

4.1 Chemicals and solutions

In order to investigate internal corrosion inhibition of carbon steel structure in sea-water, sodium caprylate (purity $\geq 99\%$, Sigma-Aldrich, product no. C5038) was used as chemical inhibitor. The corrosion test solution was 3.5wt% NaCl (artificial sea-water) prepared from sodium chloride crystals (purity $\geq 99\%$, Sigma-Aldrich, product no. C5886). In order to prepare the inhibition media, different concentrations of SC in artificial sea-water was prepared by dissolving appropriate amount of SC in the test solution. All aqueous solutions were prepared using deionized/nano pure water.

4.2 Substrate Pretreatment

The substrates were made out of a 1.59 cm diameter easy-to-machine 1117 carbon steel (CS) rod (McMaster-Carr, product no. 8290T14), machined into 3.18 mm thick coins (see Table 4.1 for the chemical composition of CS). These coupons were then degreased and thoroughly wet-polished, manually, with 600 grit silicon carbide polishing paper (from Anamet) to give a mirror-like surface. For each experiment, the button-shaped substrate was sonicated in anhydrous ethanol for ~ 5 minutes to remove residues from the polishing exercise. Then, the coin was thoroughly (but quickly) rinsed in nano pure water for about 5 seconds and immediately carefully dried with Argon at 5psi to quickly flush out the nano pure water from the surface of rinsed coin, so as to prevent the sample from swiftly forming corrosion products. The electrode is then immersed in the electrolyte and equilibrated for 2 hr at open-circuit potential (OCP), followed by a specific type of experiment conducted.

4.3 Experimental set up

A conventional 3-electrode electrochemical cell was used in all electrochemical experiments reported in the thesis. The reference electrode (RE) used was Ag/AgCl (Fisher Scientific, product no. 1362053). A graphite rod was used as the counter electrode (CE). The working electrode (WE) was the coin-shaped CS substrate (see Table 4.1 for the chemical composition of the steel). The WE was placed in a commercial WE sample holder (Princeton Applied Research, product no. K0105), which exposed a CS geometric surface area of 0.785 cm^2 to the electrolyte (Note: all the surface-area-dependent values reported in the thesis, such as current, impedance, resistance, and capacitance, were normalized with respect to the geometric surface area of the electrode). Argon was bubbled through the cell for 45 minutes prior to measurements and also during the experiment to ensure oxygen-free environment and a well-mixed bulk solution.

Once the electrodes were prepared and the cell was set up, it was connected to the potentiostat and electrochemical measurements were carried out (see Figure 4.1). All the measurements were performed at $296 \pm 2 \text{ K}$.

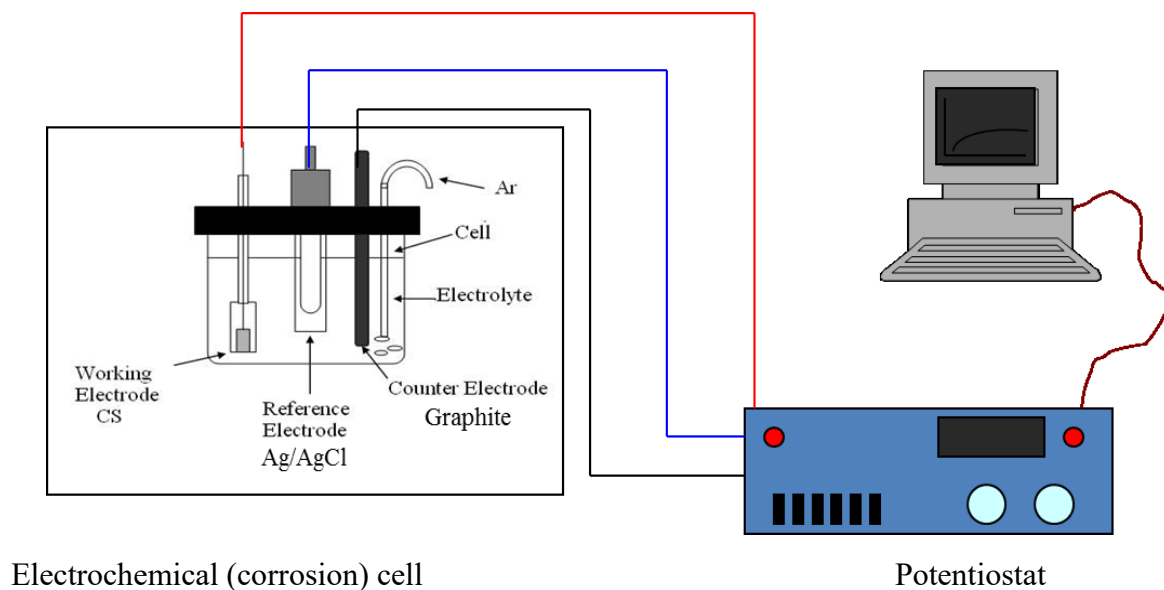


Figure 4. 1: Experimental setup

Table 4. 1: Chemical composition of carbon steel rod.

Element	Composition (wt.%)
Carbon	0.14-0.20
Manganese	1.00-1.30
Phosphorus	0.00-0.04
Sulfur	0.08-0.13
Iron	Balance

4.4 Experimental Techniques and Equipment

The proceeding text will give a summary on the fundamentals of the electrochemical experimental techniques employed and highlight the equipment sets used to achieve this. For the electrochemical techniques, emphasis will be on small amplitude cyclic voltammetry and electrochemical impedance spectroscopy (EIS), since these two techniques were used to determine the polarization resistance of the bare and protected CS working electrode; the reader can consult the literature regarding principles of the remaining experimental techniques used in the current research to characterize the electrode surface topography/morphology/structure and chemistry. The following techniques were used: open circuit potential (OCP), small amplitude cyclic voltammetry (SACV), electrochemical impedance spectroscopy (EIS), Tafel polarization (TP), and scanning electron microscopy (SEM).

4.4.1 Experimental Techniques

4.4.1.1 Open Circuit Potential (OCP)

OCP, in the context of current project, represents a corrosion potential ($E_{corr.}$) of the working electrode comparative to the reference electrode when there is no current flowing through the cell. Namely, at OCP, anodic and cathodic reactions proceed at an equal finite rate resulting in zero net-current flow. In most electrochemical corrosion experiments, the first step is to measure the OCP with time in order to determine the point at which a steady-state corrosion rate is reached, then usually proceeding to using other electrochemical techniques for corrosion rate measurement. Relative comparison of OCP values might give an indication of corrosion susceptibility: the expectation in this project is to observe a shift towards a more positive OCP value which will be indicative of increasing corrosion inhibition.

4.4.1.2 Small Amplitude Cyclic Voltammetry (SACV)

The Small Amplitude Cyclic Voltammetry (SACV) technique, also known as the modified linear polarization method, is based on the fact that current density is a linear function of applied potential near the corrosion potential (or OCP). With the SACV technique, the value of the polarization resistance R_p can be determined from steady-state current-potential hysteresis loop (see figure 4.4.1), obtained by applying a triangular potential wave of small amplitude to the WE. The slope of the hysteresis loop determined by the tangent drawn at about zero current gives the R_p value of the electrolyte/electrode surface interface, in accordance with the Ohm law. The R_p value is inversely proportional to the corrosion rate.

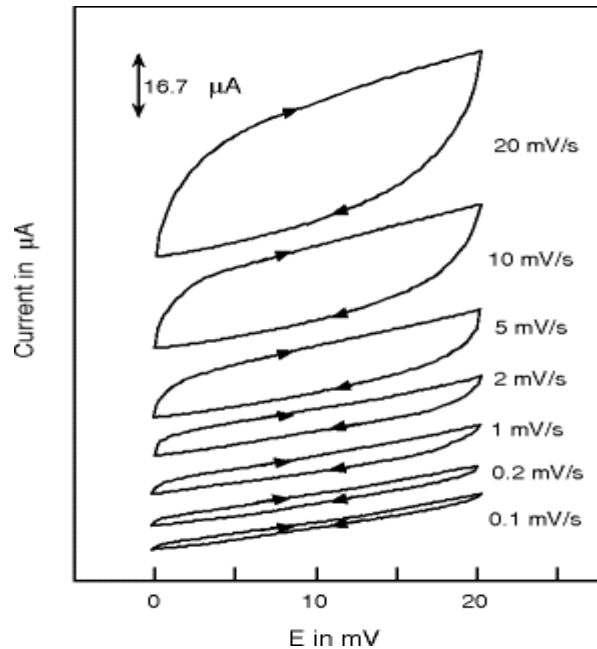


Figure 4. 2: Typical SACV current-potential loops for 90:10 Cu–Ni alloy in flowing seawater containing dissolved oxygen [35].

For this research project, the experiment scan rate was 1 mV/s. This slow scan rate was selected to ensure minimal hysteresis of the SACV loop. The potential range for the SACV was from $-10mV_{OCP}$ to $+10mV_{OCP}$, with a step potential of 0.15 mV. The scan range is to ascertain approximate linear relationship of measured current density about the OCP.

4.4.1.3 Electrochemical impedance spectroscopy (EIS)

This is a non-destructive electrochemical technique. It provides information on processes occurring at the solid-liquid interface (adsorption, charge and mass transfer, charging of the double layer, etc.) [26]. The working electrode is held at a specific *dc* potential and an *ac* sinusoidal signal of small amplitude ($\pm 5 - 10$ mV) at a certain frequency is applied over it (the excitation signal). The measured signal is *ac* current and phase angle. Impedance, which is a measure of the resistance of a circuit to a flow of electric current, can be determined for different processes due to their different time constants. Therefore, the system is scanned over a wide frequency range so as to record a response of different time constants. Then, an electrical

equivalent circuit (EEC), comprising of resistors, capacitors and inductors, is used to model the electrode/electrolyte interface and corresponding processes, thus obtaining information on the kinetics, mass transport and electric/dielectric properties. Hence, the behavior of an electrochemical system is quite similar to the behavior of an analogous electrical circuit made of real electronic elements [34].

For this work, EIS technique was applied to study the characteristics of the electrode surface/electrolyte interface and corresponding corrosion processes that takes place on the CS surface in the presence and absence of the adsorbed SC molecules. To ensure complete characterization of the interface and surface processes, EIS measurements were made at OCP in a wide frequency range, from 50 kHz to 10 mHz, with the *ac* root-mean-square voltage amplitude of ± 10 mV. The data from this measurements are very useful for monitoring corrosion rate since changes in the impedance characteristics of system are expected to occur as a function of exposure time [36]. Therefore, it is possible to predict the rate at which the CS will degrade over time, this in turn will aid better corrosion control.

4.4.1.4 Linear Tafel DC polarization

Tafel polarization is one of the most common experimental techniques used to investigate the corrosion behaviour of metallic materials because it is relatively simple to execute. The output results obtained from this method are significantly simpler to interpret than, say, EIS data. When starting a Tafel measurement, it is generally best to allow a metal electrode (i.e. WE) to reach a steady state OCP so as to obtain a more reliable data that represent a corrosion rate in nature. However, unlike EIS, this technique has been found to provide non-reliable data in case of non-linear system. It is also more destructive than EIS, therefore it is performed at the end of an EIS experiment.

In this thesis, Tafel polarization was used to corroborate EIS results, to determine kinetic parameters related to the partial corrosion reactions (iron dissolution and hydrogen evolution), and to provide information required for the determination of the corrosion inhibition mechanism.

Tafel technique is based on the linear polarization of the WE (test-sample) ca. ± 200 mV around OCP at a slow scan rate of 1 mV/s. From the recorded current response and using the electron-transfer-kinetic theory [34], kinetic parameters related to the rate of the partial and overall corrosion reaction(s) can be obtained. Tafel data provide a quick direct measure of the corrosion current, which can be related to corrosion rate.

4.4.2 Experimental Equipment

The electrochemical measurements were performed using an AUTOLAB potentiostat/galvanostat PGSTAT 30 handled by FRA2 and GPES v. 4.9 software. The surface characteristics of test samples were examined through scanning electron microscopy (Hitachi SU3500 SEM) technique.

Chapter 5: Results and Discussion

5.1 Corrosion inhibition by sodium caprylate (SC)

This section presents results on the potency of sodium caprylate (SC) as an inhibitor for CS corrosion protection, in salt-water environment. The aim of these experiments was to obtain fundamental information on the corrosion inhibition of SC on CS, and to evaluate its potential in protecting CS from general corrosion in saline environment. Hence, electrochemical measurements were made through open circuit potential (OCP), small amplitude cyclic voltammetry (SACV), electrochemical impedance spectroscopy (EIS) and Tafel polarization (TP).

It should be noted that these electrochemical corrosion measurements were performed in this sequence: an open circuit potential experiment, followed by small amplitude cyclic voltammetric measurement, then electrochemical impedance spectroscopic experiment done at OCP. Finally, a Tafel polarization (TP) experiment was carried out.

The first three experimental techniques were non-destructive to the WE, while the TP experiment was destructive as the CS surface was forced to corrode. Therefore, TP was performed last. Measurements were first done in the absence of SC in the electrolyte (control experiment), and were repeated at different concentrations of SC in the electrolyte. Note that a freshly prepared WE was always used for each experiment set.

5.1.1 Open Circuit Potential

Figure 5.1 shows the variation of open circuit potential (OCP) of CS with time in 3.5wt% NaCl solution, in the absence and presence of chosen concentrations of SC. The figure displays a common trend in OCP. The OCP values first sharply increased into the negative direction of potential, followed by semi-stabilization characterized by a small change in potential. This trend

indicates that the corrosion reaction quickly starts off as the sample is immersed in the electrolyte (mirror-like sample surface appeared blurred once sample is dipped into solution) and slows down with time, and then reaches a quasi-steady state within the time interval investigated; the shift to less noble OCP values implies increased corrosion. The plateau OCP increased to more noble values with an increase in SC concentration in the electrolyte. This is indicative of adsorption of SC on the CS surface which in turn influenced (slowed down) anodic corrosion reaction [37]. Therefore, these initial results indicate that SC can potentially act as corrosion inhibitor. To further investigate this, SACV, EIS and TP measurements were carried out in this order, as earlier explained.

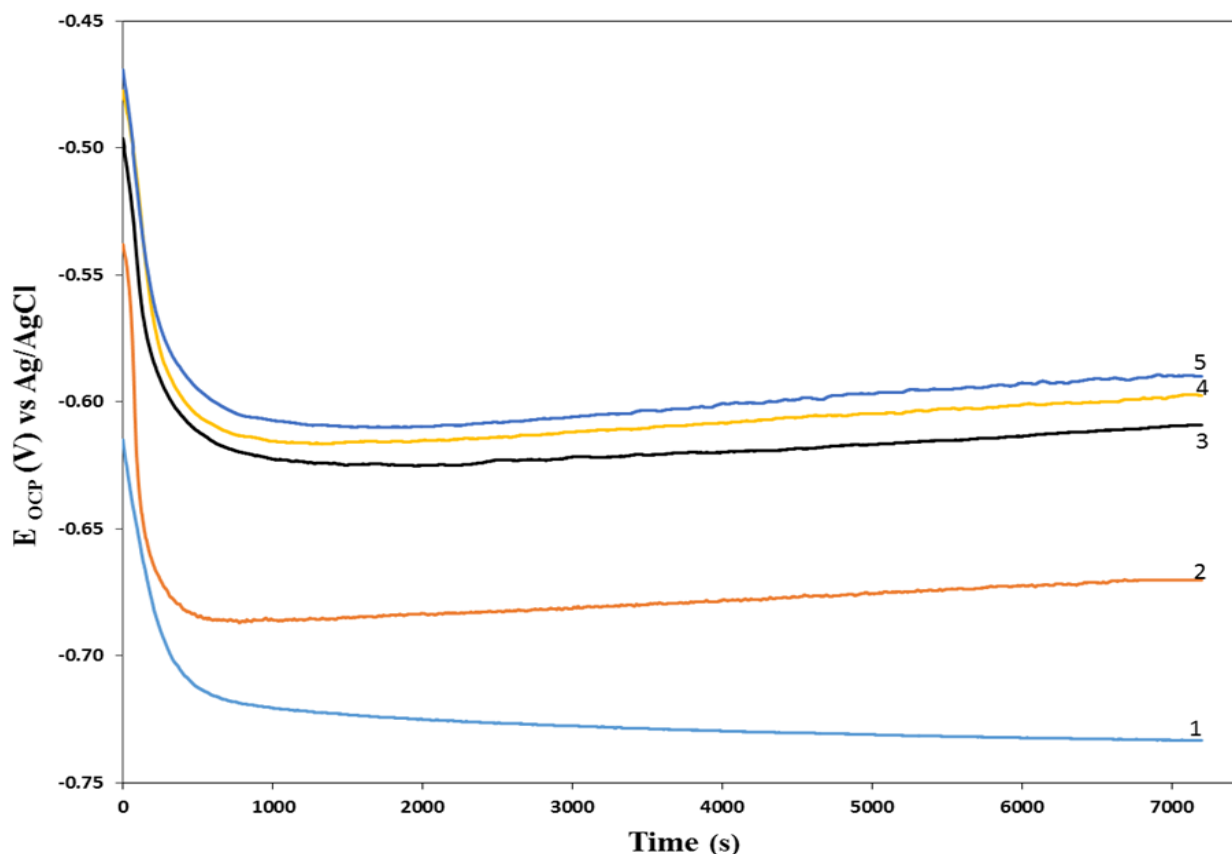


Figure 5. 1: Variation of the open circuit potential (OCP) with time for CS electrode immersed in 3.5wt% NaCl, in the absence and presence of various concentrations of SC. (1) 0 mM, (2) 20 mM, (3) 50 mM, (4) 80 mM, and (5) 100 mM SC. Temperature = 296 ± 2 K.

5.1.2 Small Amplitude Cyclic Voltammetry (SACV)

In the SACV measurements, a triangular potential perturbation signal of $\pm 10\text{mV}_{\text{OCP}}$ amplitude was applied to the WE at a slow scan rate of 1mV/s . This action ensures a semi-steady-state current-potential loop (see Figure 5.2a) is generated with minimal hysteresis. The scan range of $-10\text{mV}_{\text{OCP}}$ to $+10\text{mV}_{\text{OCP}}$ around the OCP also ensures that more linear relationship is achieved between measured current density j (A/cm^2) and potential E (V). The polarization resistance R_p is determined from the SACV loop by calculating the slope of the tangent [35, 38] taken around the open circuit potential (in accordance with Ohm's Law) and the average value of the forward and backward going scan is taken into account. As it can be seen in Figure 5.2a, the relationship between the current density and applied potential is indeed fairly linear around the OCP, making it possible to calculate the corresponding polarization resistance.

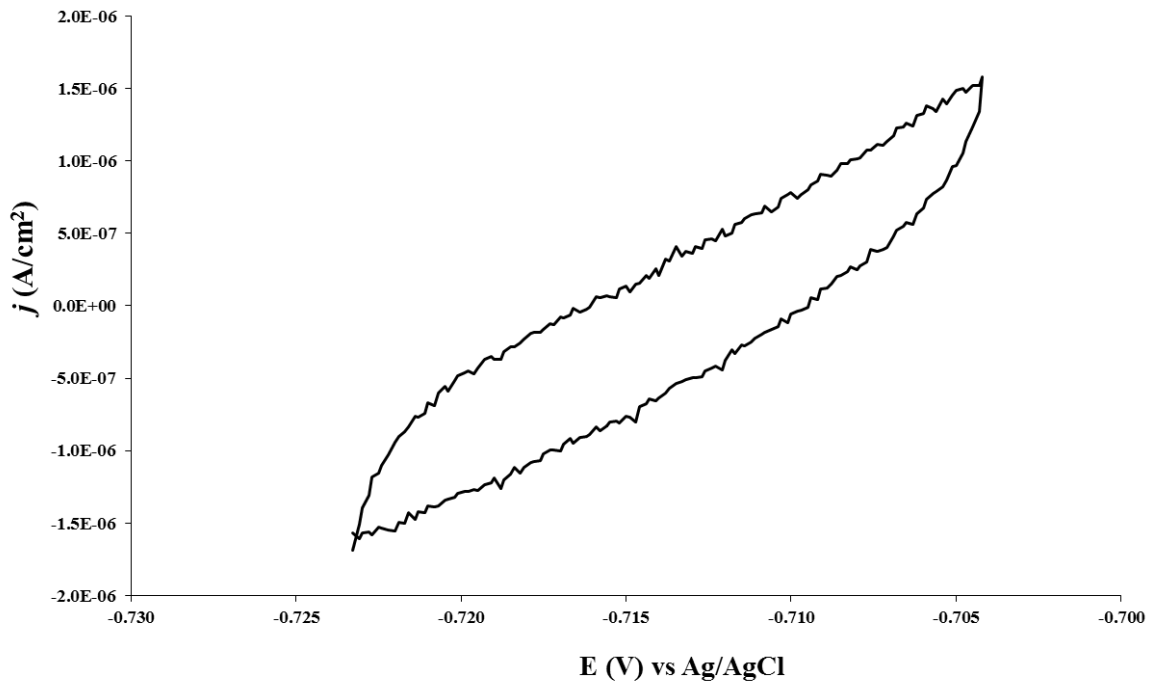


Figure 5. 2a: Typical SACV current-potential voltammogram of a CS electrode in a saline environment at 296 ± 2 K.

From Figure 5.2b, it is clear that with an increase in SC concentration in the electrolyte, the SACV slope changes and the OCP also shifts to more positive anodic potential values. The decrease in the slope implies an increase in R_p values as the concentration of SC in the electrolyte increases, indicating an increased corrosion protection. Table 5.1 lists R_p values determined from SACV measurements performed at various SC concentrations in the electrolyte.

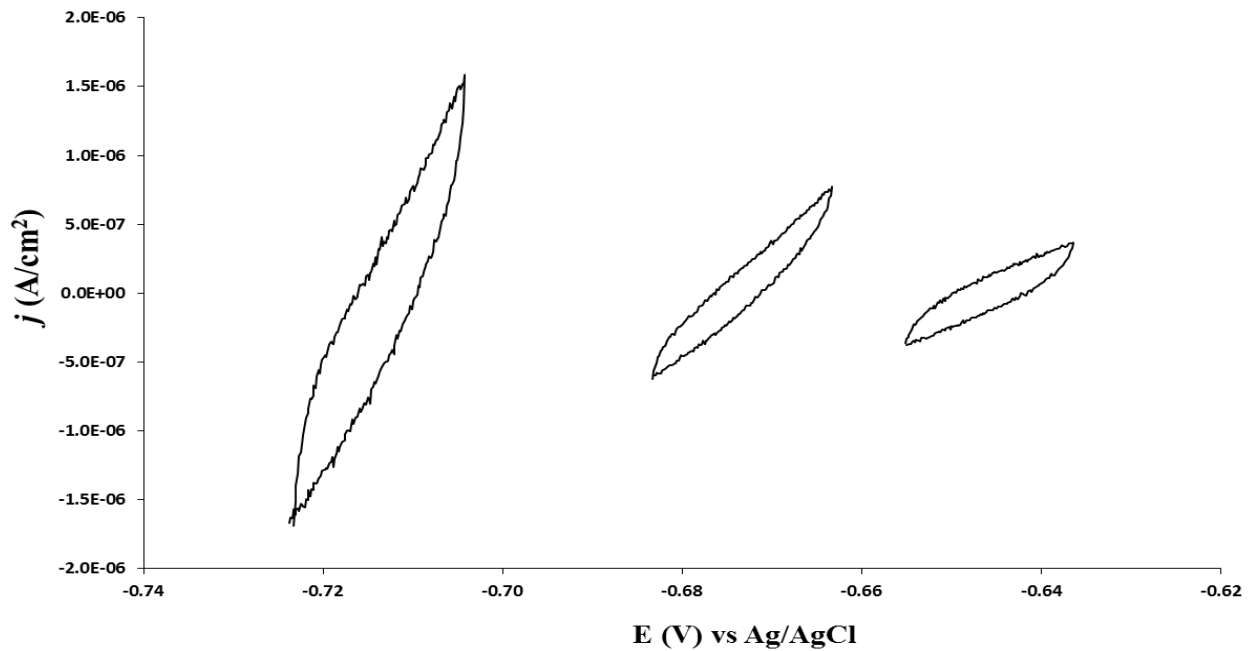


Figure 5.2b: SACV voltammograms of a CS electrode immersed in a 3.5wt% NaCl solution in the absence and presence of different concentration of SC at 296 ± 2 K: (1) 0 mM, (2) 10mM, (3) 50 mM.

Table 5. 1: OCP and polarization resistance values determined from SACV measurements performed with CS electrode in 3.5 wt% NaCl solutions without and with various concentrations of SC at 296 ± 2 K. The table also shows the corresponding corrosion inhibition efficiency.

Conc (mM)	OCP (V)	$R_p \times 10^{-3}$ (Ω)	ε (%)	ε_{std} (%)
0	-0.74	8.0		
2.5	-0.73	8.8	9	2.4
5	-0.73	11.1	28	2.4
10	-0.68	16.3	51	1.4
15	-0.68	19.4	59	1.1
20	-0.65	19.7	59	0.9
30	-0.61	20.5	61	1.2
40	-0.61	21.1	62	1.5
50	-0.60	21.6	63	1.7
60	-0.61	22.9	65	2.2
80	-0.59	34.1	77	2.7
100	-0.57	35.3	77	2.4
120	-0.57	36.3	78	1.1
140	-0.54	37.1	78	1.2

Since R_p is inversely proportional to corrosion rate, therefore the addition of the inhibitor led to corrosion mitigation. The corrosion inhibition efficiency (ε %) of SC can be obtained from equation (5.1) below by measuring the polarization resistance ($R_{p,0}$) in the absence of SC and its polarization resistance ($R_{p,i}$) in the presence of SC.

$$\varepsilon = \left(1 - \frac{R_{p,0}}{R_{p,i}}\right) \times 100\% \quad (5.1)$$

As can be seen from Table 5.1, the polarization resistance increases as the concentration of SC increases, and thus also the corresponding corrosion inhibition efficiency. The values of the standard deviation (ε_{std}) of the inhibition efficiency from this table shows the consistency of the result obtained.

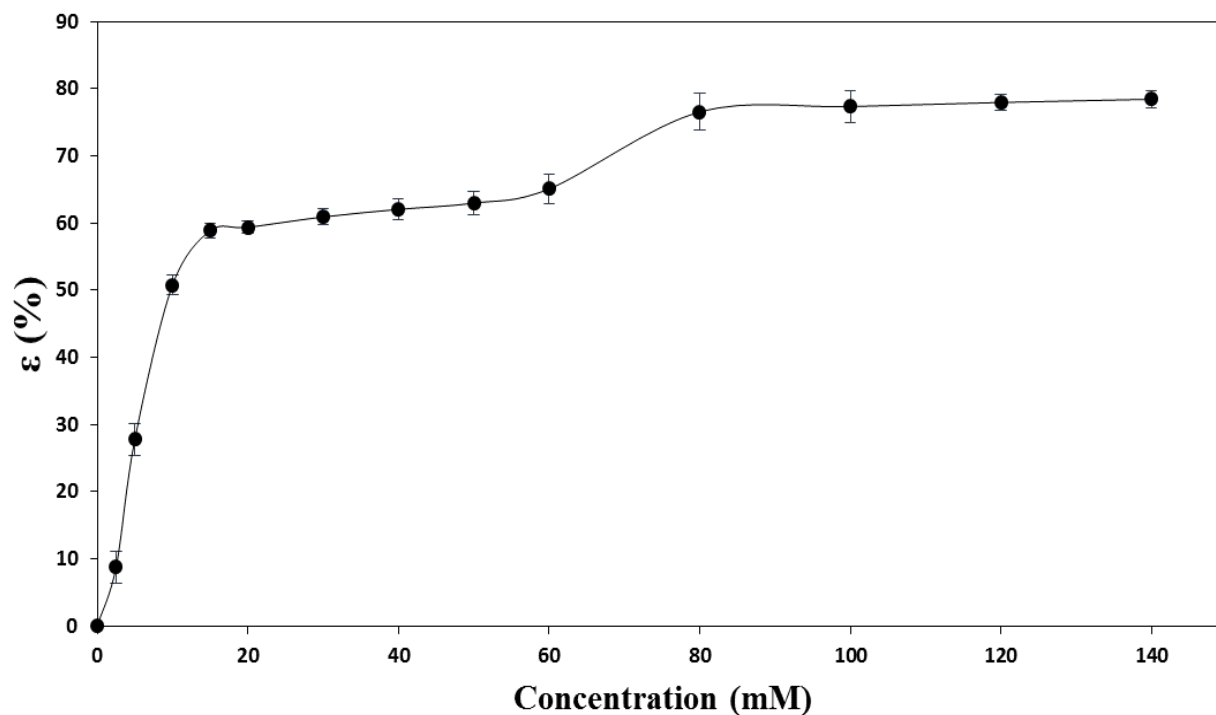


Figure 5. 3a: Corrosion inhibition efficiency of CS derived from SACV measurements performed at various concentrations of SC in 3.5wt% NaCl solution. The data was obtained at 296 ± 2 K.

From the efficiency plot of Figure 5.3a, it was observed that the inhibition efficiency increases sharply to ca. 60% at about 20mM concentration of SC. It then plateaus around that value up to 60mM concentration of SC. The efficiency increases then further with increase in concentration of sodium caprylate in the electrolyte, up to about ca. 78% forming a second plateau maintained up to 140mM SC.

It would also be interesting to examine the behaviour of OCP with SC concentration, presented in Table 5.1. Figure 5.3b shows the OCP trend recorded at various concentrations of the inhibitor in electrolyte. The plot demonstrates a trend similar to that in Figure 5.3a, confirming that OCP could also be used as an indication of corrosion protection by inhibitors, at least under the current experimental conditions.

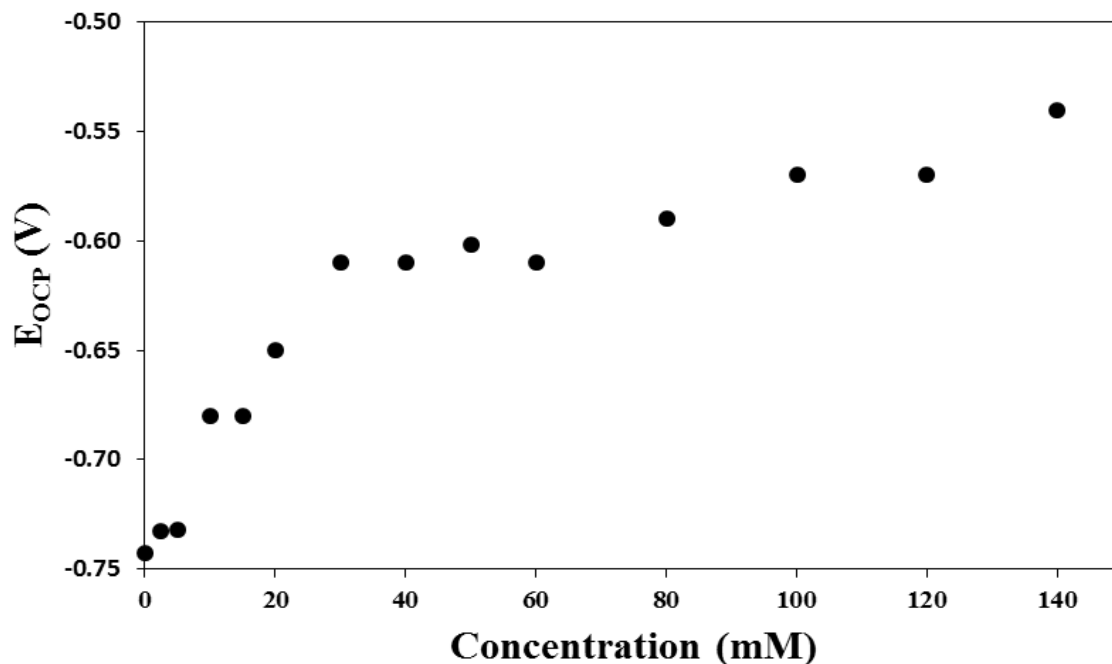


Figure 5.3b: OCP of CS as a function of SC concentration in 3.5wt% NaCl solution. The data was obtained at 296 ± 2 K.

The data presented in Table 5.1 and Figure 5.3 strongly support the claim that SC is a good corrosion inhibitor for CS in salt water since its maximum corrosion inhibition efficiency can be as high as ca. 80%. As it will be shown in the proceeding sections of the thesis, this claim was further substantiated by impedance spectroscopy and Tafel polarization measurements.

5.1.3 Electrochemical impedance spectroscopy (EIS)

Electrochemical impedance spectroscopy measurements were done to characterize the electrode/electrolyte interface and the accompanying corrosion processes that occur on the CS surface at OCP in the presence and absence of SC in the saline test solution. To better characterize the system, the impedance measurements were made over nine frequency decades, from 50 kHz to 10 mHz with *ac* root-mean-square voltage amplitude of ± 10 mV. Figure 5.4 shows the EIS spectra of the CS electrode recorded in the absence and presence of SC at different concentrations. The

figure is a plot of imaginary component of impedance ($-Z''$) versus the real component of impedance (Z') for each excitation frequency, and the plot is called a “Nyquist” or a “complex” impedance plot.

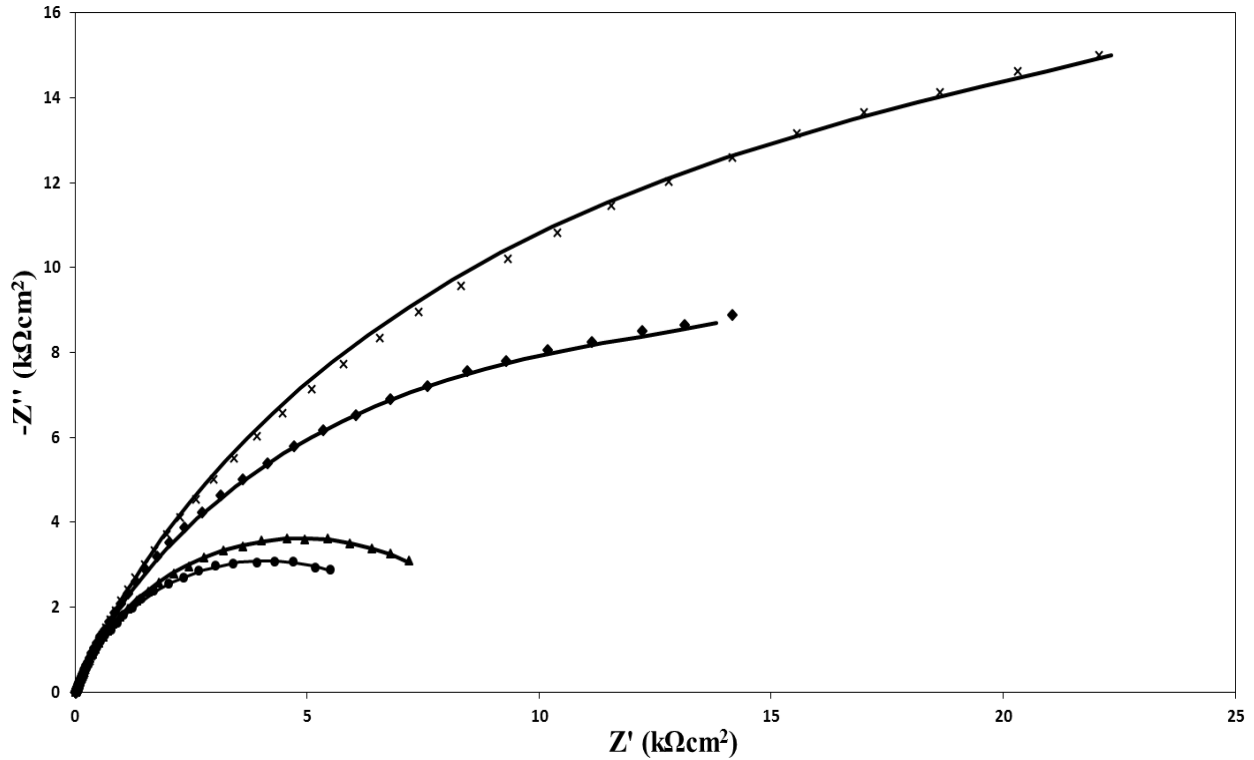


Figure 5. 4: Nyquist plot of CS recorded at different SC concentrations in 3.5wt% NaCl solution. (●) 0 mM, (▲) 5 mM, (◆) 50 mM and (x) 140 mM SC. Symbols represent experimental data and solid lines depict the modeled spectra. The spectra were recorded at OCP after 2 hours of stabilization of the CS electrode at OCP. Temperature = 296 ± 2 K.

Figure 5.4 shows that the diameter of the semicircle increased with increasing inhibitor concentration, which is indicative of increased corrosion resistance of the material in the presence of SC. With the Bode modulus impedance plot presented in Figure 5.4, one can see that there exist three distinct frequency-dependent segments. At zero concentration of SC in the high-frequency region (\geq ca. 0.8 kHz, and the region close to the origin on the Nyquist plot in Figure 5.4), the absolute impedance curve appears to be almost independent of frequency. This kind of response is

typical of resistors. The resistive behaviour can be attributed to the solution resistance between the WE and RE [39, 40]. For the medium frequency range (ca. $40 \text{ mHz} \leq f \leq 0.8 \text{ kHz}$), an approximate linear logarithmic relationship is observed between the absolute impedance and the frequency. This region is believed to correspond to the capacitive behavior of the electrode/electrolyte interface and it is referred to as the electrochemical double-layer capacitance [24, 39, 40]. The low-frequency region (\leq ca. 40 mHz and the most right points on the Nyquist plot in Figure 5.4) again shows the onset of resistive behaviour. This frequency region corresponds to the charge-transfer or polarization resistance [24], which is a direct measure of the CS corrosion rate as shown in the preceding section of the thesis. On the Nyquist plot (Figure 5.4), these regions are characterized by curves whereby the region closest to the origin is the high frequency segment while the region furthest away from the origin depicts the low frequency segment. Based on this these EIS observations, the uninhibited corroding system seems to display a one-time-constant behaviour, and can, thus, be described by the electrochemical equivalent circuit show in Figure 5.7a.

However, in the presence of SC, the EIS behavior of the system changes. At 5 mM concentration of SC, the shape of the Bode modulus spectra (Figure 5.5) was similar to that of the non-inhibited sample, but had larger magnitude of impedance as a result of increased charge-transfer resistance. This is reflected by the increase in the diameter of the Nyquist plot as shown in Figure 5.4. Therefore, the presence of SC reduced the corrosion of CS in the solution. Larger impedance values were recorded as the concentration of SC continue to increase (note the increase in a semi-circle diameter in Figure 5.4 and a shift of curves in Figure 5.5 to higher impedance modulus values). However, not only did the impedance values change at higher CS concentrations, but one can clearly observe on the Bode plot (Figure 5.5) the appearance of a second time constant at higher frequency range (ca. $0.3 \text{ kHz} \leq f \leq 23 \text{ kHz}$) for concentration greater

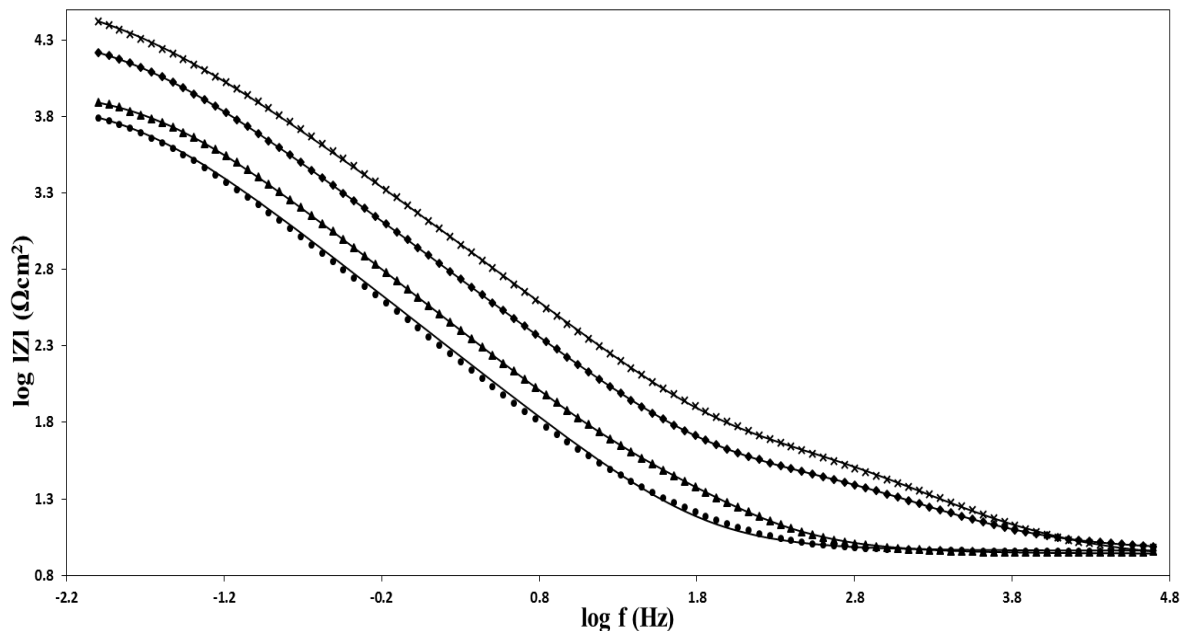


Figure 5. 5: Bode modulus impedance plots for CS recorded at various concentration of SC in the electrolyte and at OCP: (●) 0 mM, (▲) 5 mM, (◆) 50 mM and (x) 140 mM SC. Temperature, $T = 296 \pm 2$ K. Symbols represent experimental values, while solid lines depict simulated spectra.

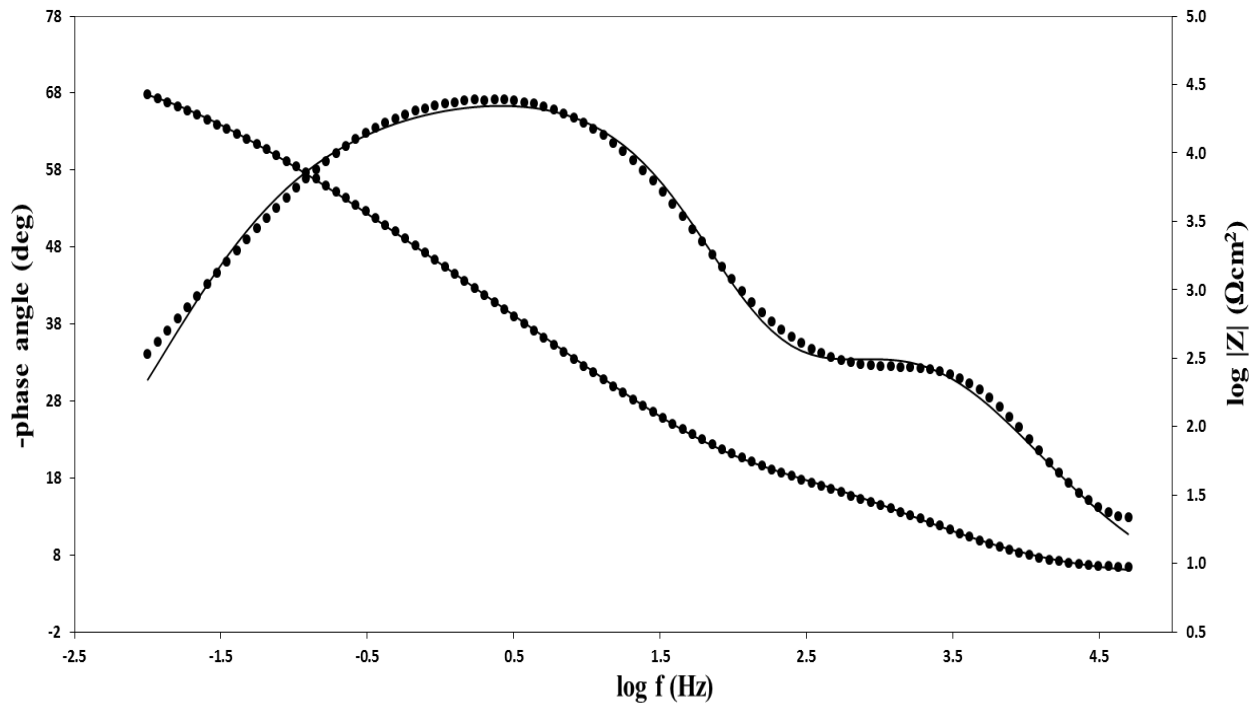


Figure 5. 6: Bode plot for CS recorded at OCP in a 140mM SC solution of 3.5wt% NaCl measured at temperature, $T = 296 \pm 2$ K. Symbol (●) represent experimental values, while the solid line (—) depicts simulated spectra.

than 5mM SC. This is even more visible in Figure 5.6 which also shows the phase angle trend, clearly displaying overlapped ‘peaks’, indicative of the presence of two time constants. This second time constant represents the impedance response of the SC layer adsorbed at the CS/electrolyte interface.

These qualitative information from the impedance spectra can be further quantified by considering the electrode/electrolyte interface and its accompanying corrosion processes at the CS surface as an electrochemical equivalent circuit (EEC). Taking into account the previous discussion on the presence of one and two time constants, and by using a nonlinear least-square fit analysis (NLLS) software [41, 42] the EECs presented in Figure 5.7 were employed to model the experimental spectra. In these EECs, R_{el} represents the ohmic (electrolyte) resistance between the WE and RE, R_1 is the charge transfer resistance of the corroding CS surface at OCP, CPE_1 is the double-layer capacitance at the electrode/electrolyte interface, R_2 depicts the pseudo-resistance of the adsorbed SC layer, while the element CPE_2 is its pseudo-capacitance [41]. The CPE_1 - R_1 time constant depicts the impedance response of the corroding CS surface in the absence of adsorbed SC (recorded at lower frequencies), while the CPE_2 - R_2 time constant represents the response of the adsorbed SC layer (recorded at higher frequencies). Figures 5.4-5.6 demonstrate that a good agreement between the experimental values (symbols) and the modelled values (lines) was achieved when the two EEC models in Figure 5.7 were employed.

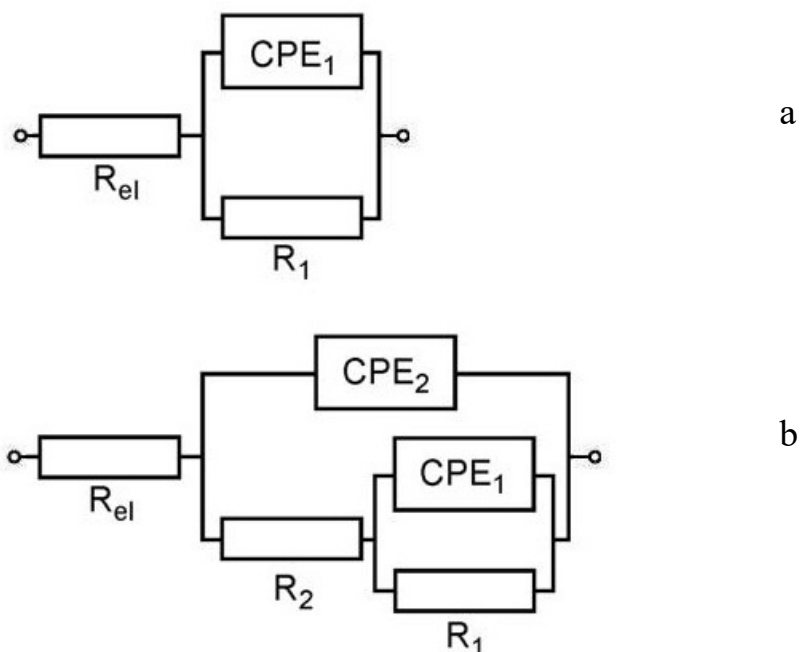


Figure 5. 7: EEC models used to fit EIS data recorded on (a) unprotected CS electrode (control sample), and (b) on a CS electrode immersed in 3.5wt% NaCl in the presence of SC. R_{el} – electrolyte resistance; CPE_1 – double-layer capacitance; R_1 – charge-transfer resistance, CPE_2 – adsorbed inhibitor layer pseudo-capacitance, R_2 – adsorbed inhibitor layer resistance.

The EEC in Figure 5.7a fitted the spectra recorded in the absence of SC in the solution. However, this model did not give a good fit for the spectra recorded in the presence of SC (especially for values at high frequency). This was due to the presence of the second time constant as a results of adsorbed SC on the surface of CS. Therefore, the two-time-constant EEC, Figure. 5.7b, was used. The two-time-constant EEC fits the data well both at low and high frequencies, as shown in Figures 5.5 and 5.6. Parameters derived from the EIS measurements and the corresponding inhibition efficiency is given in Table 5.2 for selected concentrations of SC.

Table 5. 2: Dependence of EEC parameters on the concentration of SC in the electrolyte. The data were obtained by modeling impedance spectra recorded at different concentration of SC in test solution at 296 ± 2 K and at OCP. The table also lists the corresponding corrosion inhibition efficiency values, ε_{std} = standard deviation. The average electrolyte resistance value was 11.2 ± 0.8 Ω .

Conc. (mM)	$R_p = R_1 + R_2$ (Ωcm^2)	CPE ₁		CPE ₂		ε %	ε_{std} %
		Y_0 ($\Omega^{-1}\text{cm}^{-2}\text{s}^n$)	n	Y_0 ($\Omega^{-1}\text{cm}^{-2}\text{s}^n$)	n		
0	8.14E+03	7.50E-04	0.84	-	-	-	-
10	1.32E+04	1.65E-04	0.83	1.63E-04	0.81	38	11
30	2.41E+04	1.68E-04	0.80	1.24E-04	0.74	66	2
50	2.52E+04	1.11E-04	0.81	7.96E-05	0.72	68	2
80	3.19E+04	4.87E-05	0.84	4.09E-05	0.72	74	2

The addition of SC increases the values of R_p and lowers the values of CPE and this effect is seen to be increasing as the concentrations of SC increases. Since the constant phase elements CPE₁ and CPE₂ represent the double-layer and adsorbed SC layer capacitance, respectively, the decrease in their value indicates adsorption of SC on the CS surface and an increase in the CS surface coverage by SC [24, 43]. Owing the high hydrophobicity of the SC molecule, the resulting effect is a decrease in the CS/electrolyte interfacial area, and thus a decreased corrosion rate.

As already discussed previously in the thesis, the corrosion resistance is proportional to the polarization resistance, R_p . Taking into account the physical meaning of the EEC parameters of the circuits in Figure 5.6, the corrosion resistance of the bare CS surface (control) is then equivalent to the charge-transfer resistance, R_1 , while in the presence of SC on the CS surface, the corrosion (polarization) resistance is the sum of the two resistances, $R_p = R_1 + R_2$ ($\Omega \text{ cm}^2$).

Therefore, the inhibition efficiency of the SC adsorbed on the surface of CS can be calculated as given by equation (5.1) before. The inhibition efficiency plot (see Figure 5.8) shows that with an increase in the inhibitor concentration in the bulk solution, the corrosion inhibition efficiency increases and reaches a maximum value of ca. 80% indicating high surface corrosion protection by SC molecules.

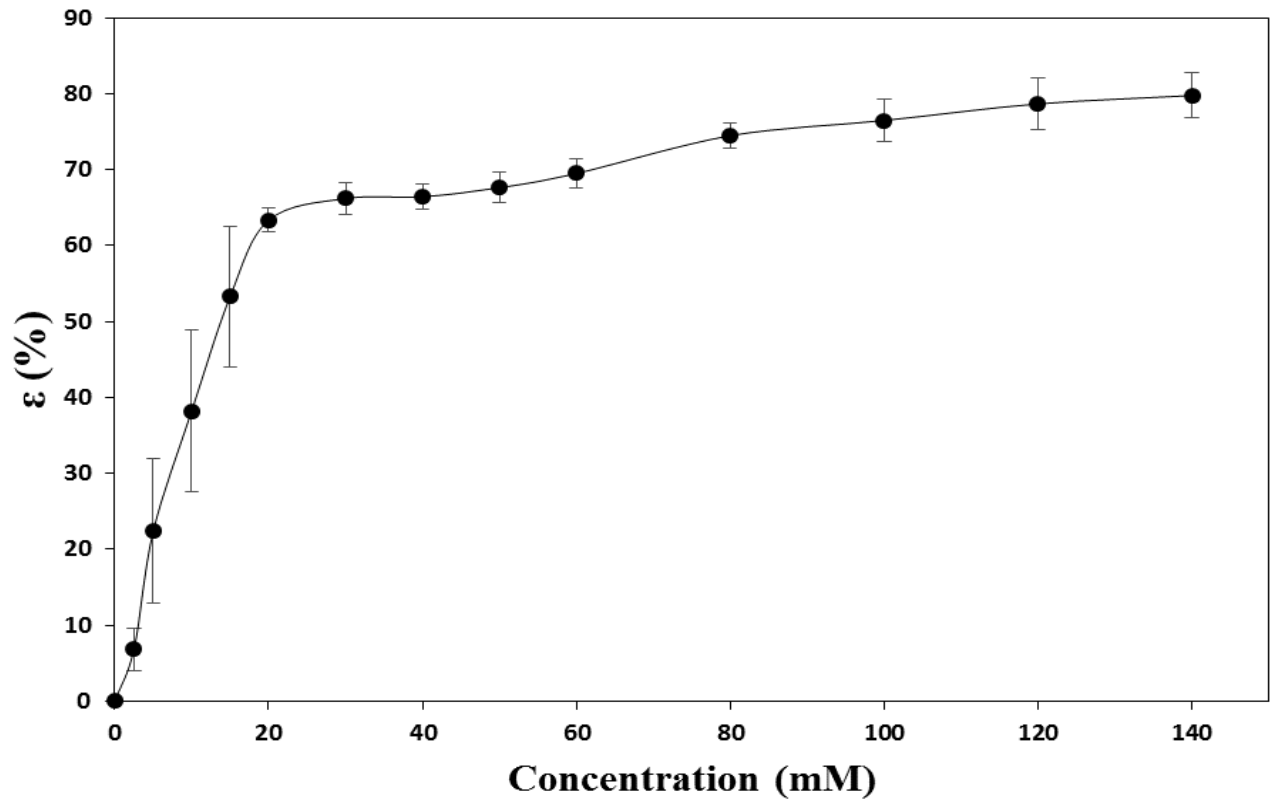


Figure 5. 8: Corrosion inhibition efficiency of CS obtained from EIS measurements performed at different concentrations of SC in 3.5wt% NaCl solution and at OCP. The data was obtained at $T=296 \pm 2$ K.

Figure 5.8 displays a trend similar to that in Figure 5.3a, indicating that SACV and EIS measurements support each other. To verify this more closely, the two trends are presented together in Figure 5.9. Indeed, the two curves are very close, confirming the validity of claims

previously made in the thesis and also the explanation of the physical meaning of EECs used to model the EIS data.

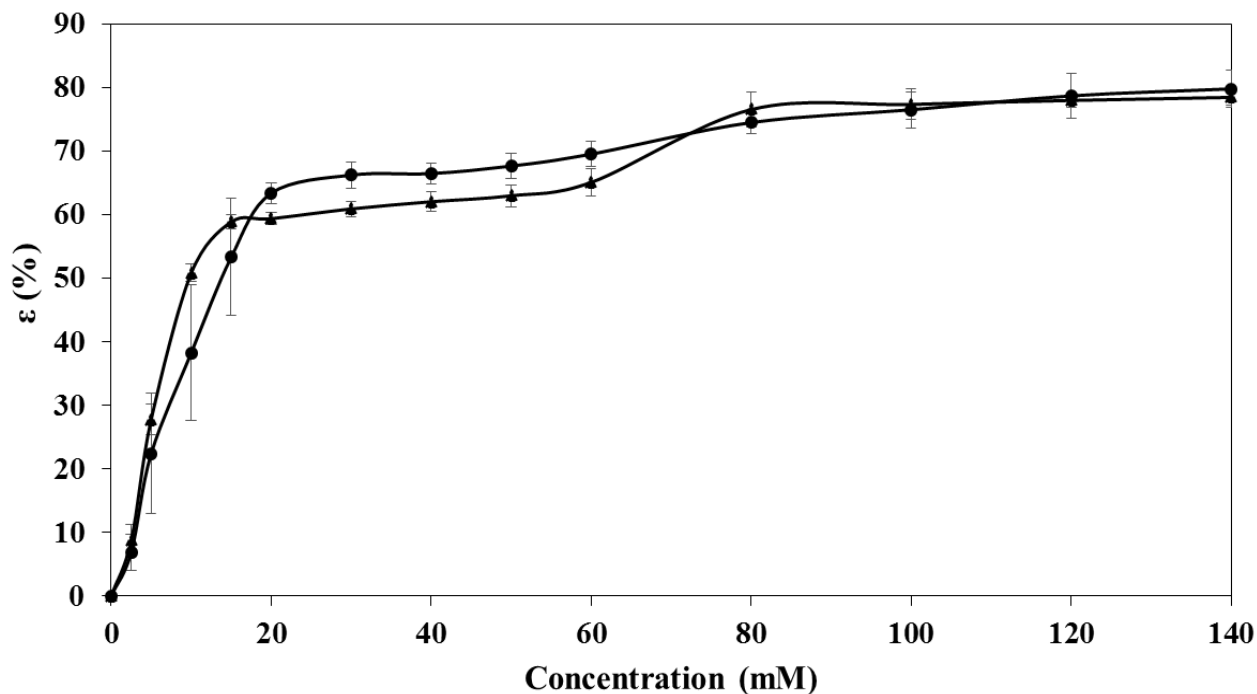


Figure 5. 9: Comparison of the inhibition efficiency of SC on CS surface immersed in a 3.5wt% NaCl aqueous solution, obtained via EIS (●) and SACV (▲) measurements at 296 ± 2 K.

5.1.3 Linear Tafel Polarization

To further verify the data obtained from EIS and SACV and gain more insight on the kinetics of partial corrosion reactions of the CS immersed in the electrolyte containing SC, Tafel polarization was carried out. This measurement was made by polarizing the WE for ± 200 mV around the OCP at a slow scan rate of 1 mV/s. Figure 5.10 represents the anodic and cathodic potentiodynamic polarization (Tafel) curves of CS in 3.5wt% NaCl solutions in the absence and presence of inhibitor in the electrolyte. Inspection of this figure reveals that the partial cathodic and anodic currents decrease in the presence of SC (when compared relative to their OCP, i.e. corrosion potential values – see Figure 5.11 for the corresponding explanation), thus

demonstrating the inhibitive effect of SC. Since the SC inhibits both partial reactions, it indicates that this inhibitor acts as mixed-type inhibitor.

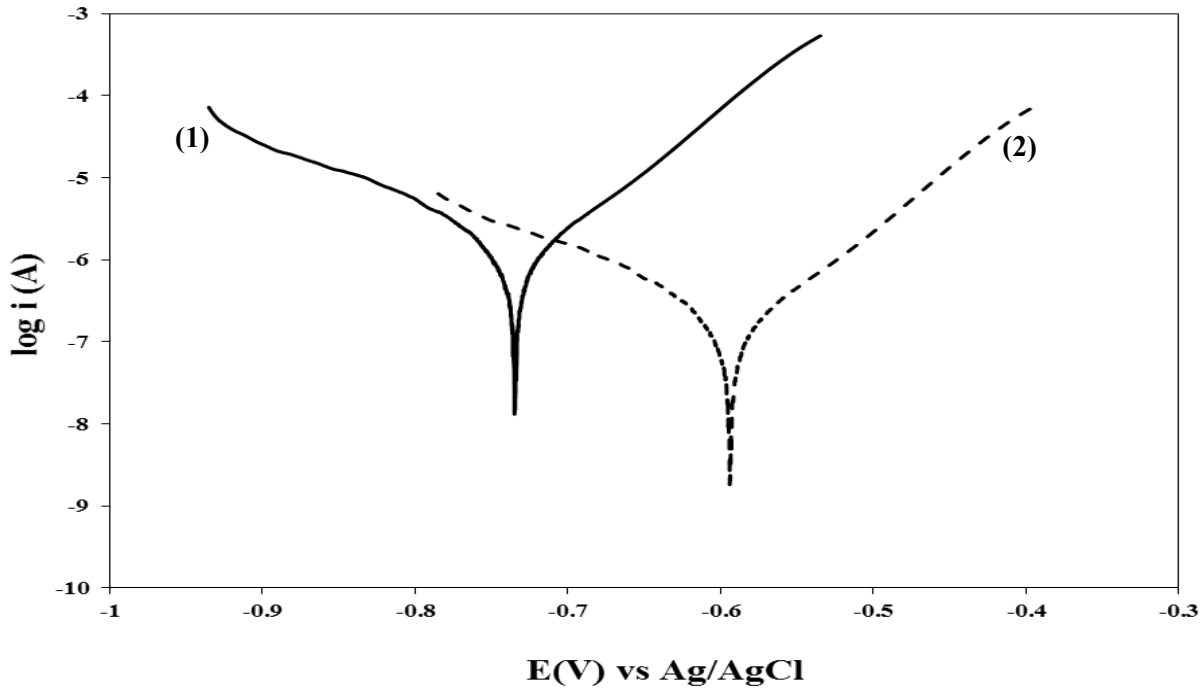


Figure 5. 10: Tafel plots of CS recorded in the (1) absence, and (2) presence of 50 mM of SC in the test solution performed at temperature, $T = 296 \pm 2$ K. Scan rate was 1 mV/s.

Tafel technique can help quantify the corrosion inhibition proffered by SC through the determination of the corrosion current, i_{corr} , which is a direct measure of corrosion rate. By extrapolating the linear part of the anodic and cathodic Tafel slopes to the corrosion potential (E_{corr} , i.e. OCP), the corrosion current can be found, Figure 5.11. The corresponding values are presented in Table 5.3. It can be seen that the corrosion current is lowered in the presence of SC. Hence the extent of inhibition provided by the SC can be qualitatively obtained by calculating the inhibition efficiency, ε , which is given by equation (5.2) below:

$$\varepsilon = \left(1 - \frac{i_{corr,i}}{i_{corr,0}} \right) \times 100\% \quad (5.2)$$

where $i_{corr,i}$ (in A) is the corrosion current at a given SC concentration, and $i_{corr,0}$ is the corrosion current of the uninhibited solution. Table 5.3 shows that the obtained inhibition efficiency results are in good agreement with the data from EIS and SACV measurements, further fortifying the validity of methods used, experiments done, and conclusions made so far.

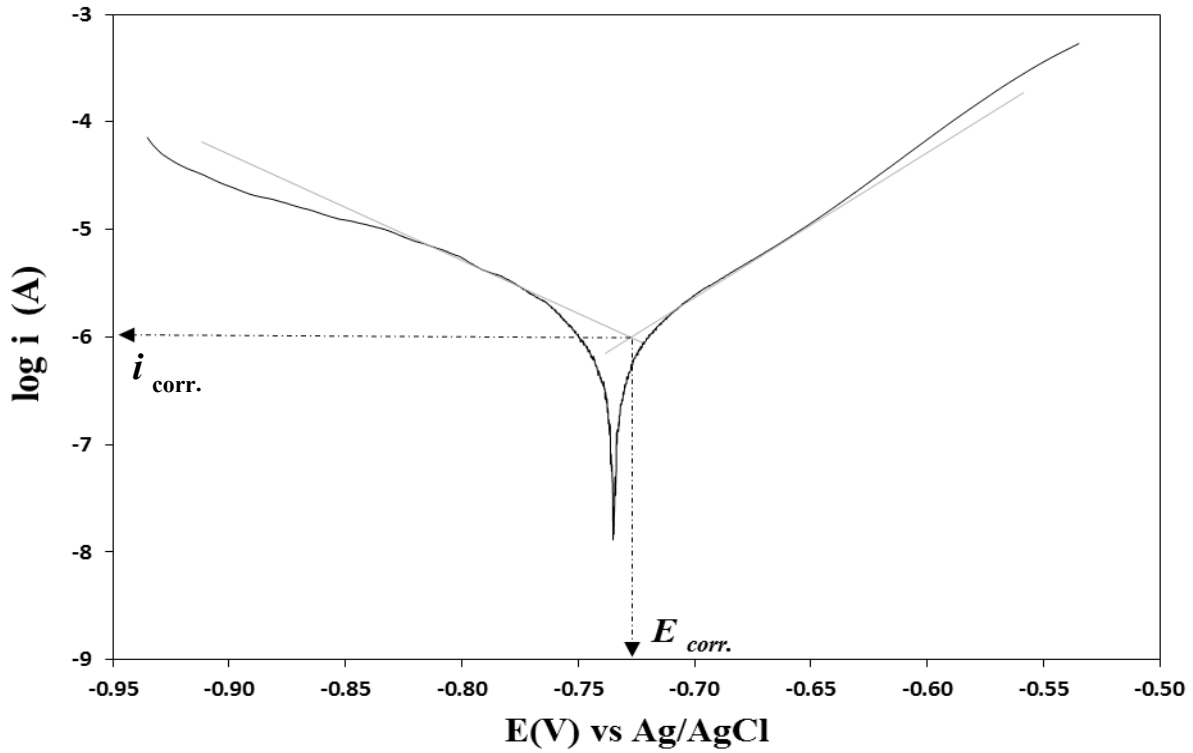


Figure 5. 11: A typical Tafel plot of CS electrode immersed in 3.5wt% NaCl illustrating the method of determining corrosion current i_{corr} .

Table 5. 3: Corrosion current values of CS in various concentration of SC in the test solution with corresponding corrosion efficiency recorded at $T = 296 \pm 2$ K.

Conc. (mM)	i (nA)	ϵ (%)
0	1031	0
10	529	49
30	379	63
50	360	65
80	224	78
140	186	82

5.1.4 SC configuration on the CS surface

The three previous sections showed that inhibition efficiency increases with concentration of SC in a peculiar manner, displaying two plateaus (see Figure 5.12 which depicts a plot obtained by combining the SACV and EIS data).

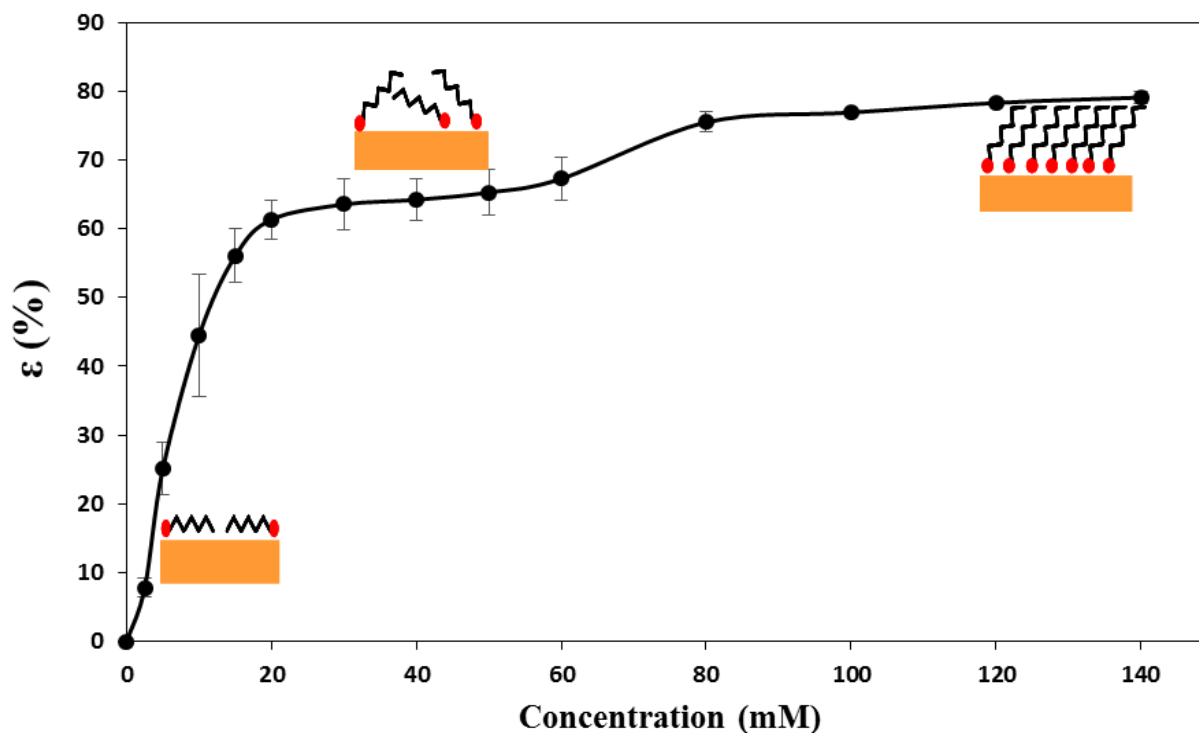


Figure 5. 12: Mean inhibition efficiency plot of CS immersed in 3.5wt% NaCl at various concentration of SC, derived from combined SACV and EIS data at temperature, $T = 296 \pm 2$ K. The inset represents the three different possible orientation of SC on the surface of CS.

The presence of two plateaus indicates that the adsorbed SC might change surface conformation with a change in equilibrium SC concentration in the bulk electrolyte, as schematically presented in Figure 5.12. The existence of the stepped curve in Figure 5.12 has been reported in the literature and was explained by Fair and Jamieson [44]. When the SC layer is formed on the CS surface, it offers a hydrophobic barrier (due to the presence of the long $-\text{CH}_2$ chain) for the penetration of solvated aggressive ions to the underlying CS surface. In this way,

corrosion of the CS surface is minimized. Corrosion inhibition efficiency is believed to be related to the surface coverage and the orientation of the SC molecules on the CS. Figure 5.12 shows that at lower concentration of SC (<30 mM), the adsorbed SC layer is thin and porous. This is because at low SC concentrations in the solution a highly disordered amorphous sub-monolayer is formed on the CS surface. This porous layer enables interaction of the corrosive electrolyte with the CS surface.

However, with a further increase in the inhibitor concentration in the bulk solution, the SC equilibrium surface concentration and coverage increase. Due to the van der Waals interactions of the neighboring $-\text{CH}_2$ chains, the orientation of SC molecules on the surface becomes more ordered. Subsequently, the orientation of the monolayer is improved, thereby, offering a tighter hydrophobic barrier (due to the presence of the long $-\text{CH}_2$ chain) for the penetration of solvated ions to the underlying CS surface. The consequence of this, is, increased corrosion inhibition efficiency. This is reflected in the further increase in corrosion inhibition efficiency to the second plateau (conc. > 80 mM SC). Hence, it can be concluded that the surface coverage and orientation of SC and on the CS surface has direct influence on the corrosion inhibition efficiency.

5.1.5 SC adsorption isotherm and kinetics of SC adsorption

5.1.5.1 Adsorption isotherm

The results presented so far evidence that the corrosion protection efficiency of SC comes from the CS surface-blockage mechanism. In other words, SC forms an adsorbed hydrophobic mono-layer on the CS surface, thus “insulating” the CS surface from the corrosive electrolyte. The corrosion inhibition efficiency was shown to depend on the bulk electrolyte concentration of SC. The corrosion inhibition efficiency vs. SC bulk solution concentration trend (Figure 5.12) displays

a typical adsorption isotherm shape. Consequently, it would be interesting to describe the SC/CS adsorptive interactions using an adsorption isotherm and to evaluate the corresponding thermodynamic data.

Thus, (i) assuming that the fractional surface coverage by SC is proportional to the corrosion inhibition efficiency, ε , (ii) taking into account only the experimental data until the end for the first plateau (Figure 5.12), and (iii) assuming that the corrosion inhibition efficiency at the SC bulk concentration of 60 mM (end of the first plateau), $\varepsilon_{60\text{mM}}$, results in a 100% surface coverage by SC, we can write that the fractional surface coverage by SC, θ , is:

$$\theta = \varepsilon / \varepsilon_{60\text{mM}} \quad (5.3)$$

and one can attempt to describe the θ vs. concentration behaviour using an adsorption isotherm. Considering the data in Figure 5.12, attempts were made to fit the data by various isotherm models, but the best agreement was obtained when the Langmuir adsorption isotherm was employed:

$$\theta = \frac{B_{ads}c}{1+B_{ads}c} \quad (5.4a)$$

or in a linearized form:

$$\frac{c}{\theta} = c + \frac{1}{B_{ads}} \quad (5.4b)$$

where B_{ads} represents the adsorption affinity constant (in dm^3/mol) and c is the inhibitor concentration (in mol/dm^3).

Taking into account experimental points from Figure 5.12 and employing Equation (5.4b), the SC surface adsorption data is presented in Figure 5.13. As evidenced, a very good agreement between the experimental data (symbols) and the adsorption model (line) is obtained ($R^2 = 0.999$).

In addition, the corresponding slope value is close to one (0.97), which is in agreement with Eq. (5.4b). Hence, the Langmuir isotherm was deemed applicable in describing the adsorption of SC onto the CS surface.

The intercept of the plot line in Figure 5.13 gives $B_{ads} = 357 \text{ dm}^3/\text{mol}$, and the corresponding apparent Gibbs free energy of adsorption was calculated from Eq. (2.3) as -23.8 kJ/mol . This means that the adsorption of SC on the CS surface is highly spontaneous. An inhibitor is considered to be good if its Gibbs free energy of adsorption more negative than -10 kJ/mol . Therefore, SC is a very good inhibitor for mitigation of the corrosion of CS in a saline environment.

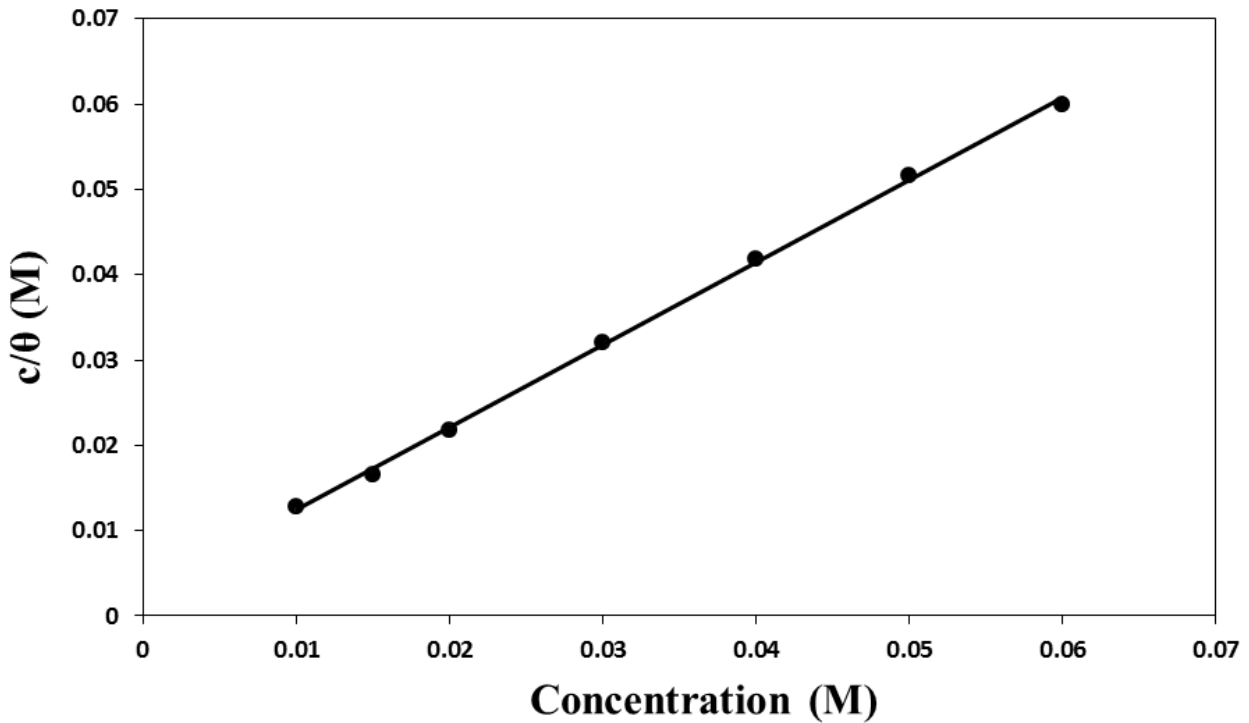


Figure 5. 13: Linearized Langmuir adsorption isotherm for the adsorption of SC onto CS surface in a 3.5wt% NaCl solution. The data was recorded at $T= 296 \pm 2 \text{ K}$.

5.1.5.2 SA adsorption kinetics

Since the Langmuir isotherms has demonstrated to be appropriate for modeling the equilibrium adsorption data of SC on CS, the adsorption of SC can be considered to follow a first-order kinetics. Consequently, the corresponding kinetic model can be described as [45]:

$$\frac{d\theta}{dt} = k_a c(1 - \theta) - k_d \theta \quad (5.5)$$

where the equilibrium adsorption constant can be related to the two rate constants as:

$$B_{ads} = \frac{k_a}{k_d} \quad (5.6)$$

where k_a is the adsorption constant (in $\text{dm}^3/\text{mol}\cdot\text{s}$) and k_d is the desorption constant (in s^{-1}). The integral version of Eq.(5.5) is:

$$\theta = \frac{k_a c}{k_a c + k_d} [1 - \exp(-(k_a c + k_d)t)] \quad (5.7)$$

Figure 5.14 presents the variation of surface coverage with adsorption time recorded around OCP by SACV in 80 mM SC in artificial sea-water. Note: the surface coverage was calculated in a similar way as surface coverage in equilibrium adsorption experiments. Namely, the inhibition efficiency was first determined from two set of time-dependent measurements of R_p , one in the absence of inhibitor (control) and the other in the presence of inhibitor in the solution. The ratio of the two was used to calculate the corresponding inhibition efficiency according to Eq. (5.1) and then the fractional surface coverage was calculated from the ratio of inhibition efficiency at various time and the maximum inhibition efficiency (at the last time point measured). This assumes that at 80 mM of SC in the solution, the surface coverage by SC is 100%.

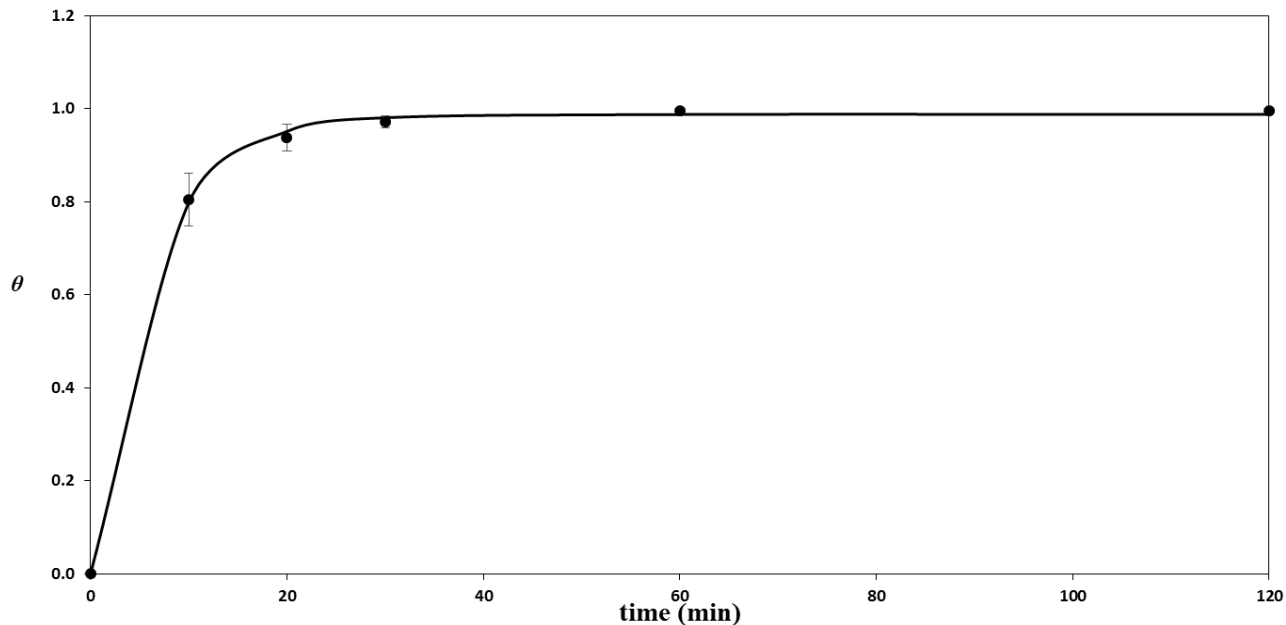


Figure 5. 14: SC fractional surface coverage on CS obtained from SACV experiments performed in 3.5wt% NaCl solution containing 80 mM of SC, at 296 ± 2 K. Symbols represent experimental values, while the solid line represents the kinetic model, Eq. (5.7).

The data in Figure 5.14 was modeled employing Eq. (5.7) (using the Solver module in Excel and minimizing the sum of squares of errors). The figure evidences a good fit between the two, confirming that the first-order kinetics can be used to describe the kinetics of SC adsorption on CS. The adsorption rate constant was calculated to be $2.0 \text{ dm}^3/\text{mol}\cdot\text{min}$, while the desorption constant was 2.0 min^{-1} . Then, employing Eq. (5.6) and Eq. (2.2), the apparent Gibbs free energy of adsorption was calculated to be -26.9 kJ/mol , which is close to the value obtained from the equilibrium adsorption measurements (-23.8 kJ/mol) presented before.

The data in Figure 5.14 also provides information on the time needed to reach a steady-state corrosion inhibition: under the experiment conditions performed, it takes 30 min after addition of SC in the electrolyte to reach the maximum protection efficiency at the given inhibitor concentration.

5.1.6 Scanning electron microscopy

Scanning electron microscopy (SEM) imaging was performed in order to obtain information on the morphology of the corroding CS surface in the presence and absence of SC inhibitor. Freshly prepared CS coins were immersed in the uninhibited and inhibited (50 and 140 mM) electrolyte and were allowed to corrode for 72 hours, followed by their SEM imaging, Figure 5.15.

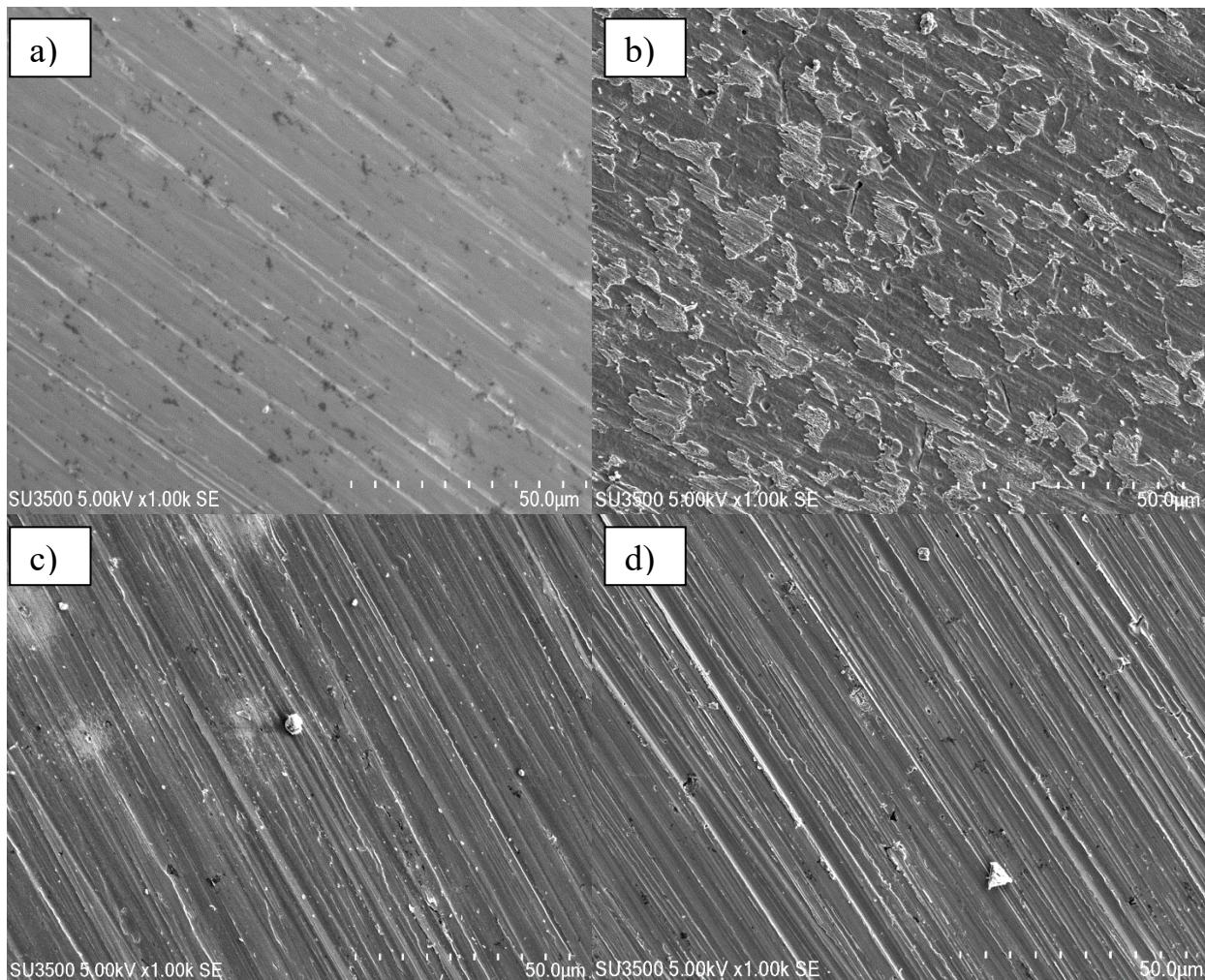


Figure 5. 15: SEM micrographs of CS surface: (a) after polishing (b) after 72h of immersion in uninhibited test solution (c) after 72h of immersion in 50mM SC (d) after 72h of immersion in 140mM SC.

Comparison of the images in Figures 5.15a and 5.15b shows that in the absence of SC inhibitor in the test solution, the extent of corrosion of CS surface was significant, as evidenced by the

presence of rust on the surface. On the other hand, when 50 mM and 140 mM of SC was present in the solution (see Figures 5.15c and 5.15d, respectively) no evidence of rust on the surface was noticed, demonstrating that SC is capable of protecting the CS surface even after 3 days of constant immersion of the CS sample in the protected solution. The scratch lines and pores were created on the CS surface during the polishing exercise.

Chapter 6: Conclusions and Future Work

6.1 Conclusions

It was shown that sodium caprylate is a good inhibitor for carbon steel in salt-water environment.

SACV, EIS and Tafel polarization measurements were first used to evaluate the efficiency of SC in the inhibition of general corrosion of CS in aqueous 3.5wt% NaCl solution, in the SC concentration range from 2.5 to 140mM. Good agreement of results produced by the three techniques was demonstrated. A maximum inhibition efficiency value of $80 \pm 2\%$ was achieved at the SC concentration of 140mM. Tafel polarization studies showed that SC inhibited both partial corrosion reactions of CS in the test solution. Therefore, SC acts as a mixed-type corrosion inhibitor.

The adsorption of SC molecules on the surface of CS was deemed responsible for the action of the inhibitor. The SC adsorption lead to the formation of a self-assembled-monolayer (SAM) on the CS surface. The adsorption process was described by the Langmuir isotherm. The apparent Gibbs free energy of adsorption was calculated to be -23.8 kJ/mol, indicating that SC adsorption is highly spontaneous.

Kinetic adsorption measurements revealed that the maximum inhibition efficiency and the SC adsorption equilibrium measured in 80mM SC solutions was achieved after 30min of adsorption. The adsorption kinetics was found to follow the first-order adsorption kinetics. The corresponding adsorption/desorption constants were used to calculate the adsorption equilibrium constant and then the apparent Gibbs free energy of adsorption (-26.9 kJ/mol), which agreed well with the value obtained from the equilibrium adsorption measurements.

SEM micrographs showed that the surface of the SC-inhibited CS was very much intact after 72 hours of exposure to the corrosive medium, while that of the uninhibited CS appeared to have deteriorated significantly.

6.2 Recommendations for Future Work

The work presented in this thesis focused on the corrosion inhibition of CS in saline environment by sodium caprylate. The information obtained is of practical relevance for the protection CS structures in the oil & gas industry. However, more studies should be done to understand the interaction of the SC/CS system at other conditions other than the inhibitor concentration variation here studied. Therefore, the author of the thesis would like to suggest the following future work to be carried out in the Omanovic laboratory:

- Investigation of the influence of alkyl chain length on the inhibitor/CS surface interactions.
- Investigate the influence of temperature, pH, and fluid flow (mimicry of offshore flow conditions) on the corrosion inhibition efficiency of SC on the CS surface.
- Investigate the performance of SC in a crude oil/salt-water mixture.
- Investigate the possibility of using other environmentally-friendly amino acid based molecules as corrosion inhibitors for CS.
- It will be good to see how SC would perform in slowing down the corrosion process of an already corroding system.
- Investigate corrosion inhibition efficiency of SC in sour and sweet corrosion which is typical in offshore crude oil exploration.
- Apply other surface characterization technique other than SEM to get better understanding of the surface interactions of SC layer with CS.

Reference

1. Everything2. *Corrosion (thing)*. 2004; Available from: <http://everything2.com/user/Professor+Pi/writeups/Corrosion>.
2. Lieser, M. and C. Stek, *Composites and the Future of Society: Preventing a Legacy of Costly Corrosion with Modern Materials*. Owens Corning, 2010: p. 1 -12
3. Villamizar, W., et al., *CO₂ corrosion inhibition by hydroxyethyl, aminoethyl, and amidoethyl imidazolines in water–oil mixtures*. Journal of Solid State Electrochemistry, 2007. **11**(5): p. 619-629.
4. Rodríguez-Valdez, L.M., et al., *Computational simulations of the molecular structure and corrosion properties of amidoethyl, aminoethyl and hydroxyethyl imidazolines inhibitors*. Corrosion science, 2006. **48**(12): p. 4053-4064.
5. Kermani, M. and A. Morshed, *Carbon dioxide corrosion in oil and gas production-A compendium*. Corrosion, 2003. **59**(8): p. 659-683.
6. Perez, N., *Electrochemistry and corrosion science*. 2004: Springer.
7. Wicks, Z.W., et al., *Corrosion Protection by Coatings*, in *Organic Coatings*. 2006, John Wiley & Sons, Inc. p. 137-158.
8. Möller, H., E. Boshoff, and H. Froneman, *The corrosion behaviour of a low carbon steel in natural and synthetic seawaters*. JS Afr I Min Metall, 2006. **106**: p. 585-592.
9. Rong, J., et al., *Solution Ionic Strength Engineering As a Generic Strategy to Coat Graphene Oxide (GO) on Various Functional Particles and Its Application in High-Performance Lithium–Sulfur (Li–S) Batteries*. Nano Letters, 2013. **14**(2): p. 473-479.
10. Dennis, R.V., et al., *Graphene nanocomposite coatings for protecting low-alloy steels from corrosion*. American Ceramic Society Bulletin, 2013. **92**(5): p. 18-24.
11. Knag, M., J. Sjöblom, and E. Gulbrandsen, *Partitioning of a model corrosion inhibitor in emulsions*. Journal of dispersion science and technology, 2006. **27**(1): p. 65-75.
12. Knag, M., *Fundamental behavior of model corrosion inhibitors*. Journal of dispersion science and technology, 2006. **27**(5): p. 587-597.
13. Popoola, L.T., et al., *Corrosion problems during oil and gas production and its mitigation*. International Journal of Industrial Chemistry, 2013. **4**(1): p. 1-15.
14. Palou, R.M., O. Octavio, and N.V. Likhanova, *Environmentally Friendly Corrosion Inhibitors*. Developments in Corrosion Protection, 2014: p. 432.

15. Revie, R.W., *Uhlig's Corrosion Handbook*. 2000, New York City, New York: John Wiley and Sons.
16. Roberge, P.R., *Handbook of Corrosion Engineering McGraw-Hill*. New York, NY, 2000.
17. El-Naggar, M., *Corrosion inhibition of mild steel in acidic medium by some sulfa drugs compounds*. Corrosion Science, 2007. **49**(5): p. 2226-2236.
18. Morad, M. and A.K. El-Dean, *2, 2'-Dithiobis (3-cyano-4, 6-dimethylpyridine): A new class of acid corrosion inhibitors for mild steel*. Corrosion science, 2006. **48**(11): p. 3398-3412.
19. Migahed, M., E. Azzam, and A. Al-Sabagh, *Corrosion inhibition of mild steel in 1 M sulfuric acid solution using anionic surfactant*. Materials Chemistry and physics, 2004. **85**(2): p. 273-279.
20. Rani, B. and B.B.J. Basu, *Green inhibitors for corrosion protection of metals and alloys: An overview*. International Journal of Corrosion, 2011. **2012**.
21. Quraishi, M. and D. Jamal, *Technical note: CAHMT-a new and eco-friendly acidizing corrosion inhibitor*. Corrosion, 2000. **56**(10): p. 983-985.
22. Moretti, G., F. Guidi, and G. Grion, *Tryptamine as a green iron corrosion inhibitor in 0.5 M deaerated sulphuric acid*. Corrosion science, 2004. **46**(2): p. 387-403.
23. Choi, D.-J., S.-J. You, and J.-G. Kim, *Development of an environmentally safe corrosion, scale, and microorganism inhibitor for open recirculating cooling systems*. Materials Science and Engineering: A, 2002. **335**(1): p. 228-235.
24. Ghareba, S. and S. Omanovic, *Interaction of 12-aminododecanoic acid with a carbon steel surface: towards the development of 'green' corrosion inhibitors*. Corrosion Science, 2010. **52**(6): p. 2104-2113.
25. Munoz, A.I., et al., *Inhibition effect of chromate on the passivation and pitting corrosion of a duplex stainless steel in LiBr solutions using electrochemical techniques*. Corrosion science, 2007. **49**(8): p. 3200-3225.
26. Omanovic, S. and S. Roscoe, *Effect of linoleate on electrochemical behavior of stainless steel in phosphate buffer*. Corrosion, 2000. **56**(7): p. 684-693.
27. de Souza, F.S. and A. Spinelli, *Caffeic acid as a green corrosion inhibitor for mild steel*. Corrosion Science, 2009. **51**(3): p. 642-649.
28. Barakat, Y., A. Hassan, and A. Baraka, *Corrosion Inhibition of mild steel in aqueous solution containing H₂S by some naturally occurring substances*. Materialwissenschaft und Werkstofftechnik, 1998. **29**(7): p. 365-370.

29. Quraishi, M. and J. Rawat, *Corrosion inhibiting action of tetramethyl-dithia-octaaza-cyclotetradeca-hexaene (MTAH) on corrosion of mild steel in hot 20% sulfuric acid*. Materials chemistry and physics, 2003. **77**(1): p. 43-47.
30. Luo, H., Y. Guan, and K. Han, *Inhibition of mild steel corrosion by sodium dodecyl benzene sulfonate and sodium oleate in acidic solutions*. Corrosion, 1998. **54**(8): p. 619-627.
31. Ashassi-Sorkhabi, H., et al., *Corrosion inhibition of carbon steel in hydrochloric acid by some polyethylene glycols*. Electrochimica acta, 2006. **51**(18): p. 3848-3854.
32. Undiandeye, J.A., et al., *Kinetics of the corrosion of mild steel in petroleum-water mixture using ethyl ester of lard as inhibitor*. African Journal of Pure and Applied Chemistry, 2014. **8**(3): p. 60-67.
33. Yurt, A., et al., *Investigation on some Schiff bases as HCl corrosion inhibitors for carbon steel*. Materials Chemistry and Physics, 2004. **85**(2): p. 420-426.
34. Ghareba, S. and S. Omanovic, *12-Aminododecanoic acid as a corrosion inhibitor for carbon steel*. Electrochimica acta, 2011. **56**(11): p. 3890-3898.
35. Macdonald, D.D., *An Impedance Interpretation of Small Amplitude Cyclic Voltammetry I. Theoretical Analysis for a Resistive-Capacitive System*. Journal of the Electrochemical Society, 1978. **125**(9): p. 1443-1449.
36. Rout, T.K., *Electrochemical impedance spectroscopy study on multi-layered coated steel sheets*. Corrosion Science, 2007. **49**(2): p. 794-817.
37. Ashassi-Sorkhabi, H. and E. Asghari, *Effect of hydrodynamic conditions on the inhibition performance of l-methionine as a "green" inhibitor*. Electrochimica Acta, 2008. **54**(2): p. 162-167.
38. Kain, R.M. and W.T. Young, *Corrosion Testing in Natural Waters: Second Volume*. Vol. 1300. 1997: Astm International.
39. Omanovic, S. and S.G. Roscoe, *Electrochemical studies of the adsorption behavior of bovine serum albumin on stainless steel*. Langmuir, 1999. **15**(23): p. 8315-8321.
40. Jackson, D.R., S. Omanovic, and S.G. Roscoe, *Electrochemical studies of the adsorption behavior of serum proteins on titanium*. Langmuir, 2000. **16**(12): p. 5449-5457.
41. Felhősi, I., et al., *Kinetics of self-assembled layer formation on iron*. Electrochimica Acta, 2002. **47**(13): p. 2335-2340.

42. Aramaki, K. and T. Shimura, *An ultrathin polymer coating of carboxylate self-assembled monolayer adsorbed on passivated iron to prevent iron corrosion in 0.1 M Na₂SO₄*. Corrosion Science, 2010. **52**(1): p. 1-6.
43. Damian, A. and S. Omanovic, *Electrochemical reduction of NAD⁺ on a polycrystalline gold electrode*. Journal of Molecular Catalysis A: Chemical, 2006. **253**(1): p. 222-233.
44. Fair, B. and A. Jamieson, *Studies of protein adsorption on polystyrene latex surfaces*. Journal of Colloid and Interface Science, 1980. **77**(2): p. 525-534.
45. Atkins, P.W., *Physical chemistry*. 1994, New York: W.H. Freeman.